AD NUMBER: AD0874266
LIMITATION CHANGES
TO: Approved for public release; distribution is unlimited.
FROM: Distribution authorized to U.S. Gov't. agencies and their contractors; Export Control; 4 Aug 1970. Other requests shall be referred to the Naval Weapons Center, Corona Labs (Code 7565), Corona, CA 91720.
AUTHORITY
USNWC LTR, 24 MAR 1972

NWC TP 4952
COPY 144

COMPARISON OF WAVEGUIDE AND WAVE HOP TECHNIQUES FOR VLF PROPAGATION MODELING

by

D. G. Morfitt
Research Department

and

R. F. Halley
Astrophysics Research Corporation

ABSTRACT. Several mathematical models for describing VLF radio wave propagation in the earth-ionosphere waveguide have been presented in the literature. The Wave Hop model and the Waveguide mode model are investigated.

The computerized versions of these propagation models are examined by comparing the computed electric field strengths obtained for each model when using the same input parameters. It is found that the two models as they now exist do not produce exactly the same computational results, and that the degree of difference between the two computations is dependent upon propagation frequency and the electron-density profile used for the ionosphere.

NAVAL WEAPONS CENTER
CHINA LAKE, CALIFORNIA • AUGUST 1970

56

NAVAL WEAPONS CENTER

AN ACTIVITY OF THE NAVAL MATERIAL COMMAND

FOREWORD

The work described in this report was conducted as part of a continuing investigation to evaluate VLF propagation modeling techniques. The work was performed in the Space Geophysics Division of the Research Department, under the sponsorship of the Defense Atomic Support Agency (DASA) (Code RAAE). Funding was provided by MIPR 543-70.

Released by
V. E. HILDEBRAND, Head
Space Geophysics Division
4 August 1970

Under authority of
H. W. HUNTER, Head
Research Department

NWC Technical Publication 4952

Published by . . . . Corona Information Division
Collation . . . . . Cover, 30 leaves, DD Form 1473, abstract cards
First printing . . . . 320 numbered copies
Security classification . . . . UNCLASSIFIED

3 September 1970

ERRATA

Naval Weapons Center. COMPARISON OF WAVEGUIDE AND WAVE-HOP TECHNIQUES FOR VLF PROPAGATION MODELING, by D. G. Morfitt and R. F. Halley. China Lake, Calif., NWC, 4 August 1970. 58 pp. (NWC TP 4952.)

Make the following pen and ink changes:

1. Page 36, Figure 13. In legend, change frequency 28.125 kHz to 15.567 kHz.

2. Page 46. Equation (3) in the summation $\sum_{j=0}^{N} E_j$, change j=0 to j=1.

CONTENTS

BLANK PAGE

INTRODUCTION

The Naval Weapons Center Corona Annex (NWCCA) has been tasked by the Defense Atomic Support Agency (DASA) to investigate, with the aid of the oblique-incidence VLF ionospheric sounder developed at the Corona Annex (see Ref. 1), the accuracy with which VLF radio-wave propagation can be predicted. This is to be accomplished by correlating the sounder signals experimentally recorded at specific locations along a propagation path with the values predicted by various existing theoretical VLF propagation models.

Several models applicable to VLF radio-wave propagation have been described in the literature. Some of these have been made available in the form of digital computer programs which provide a convenient means for obtaining full-wave calculations of VLF field strengths. An excellent summary of these existing VLF computer codes is presented in Ref. 2.

The objective of the VLF program at Corona is to determine which propagation environments can be adequately represented or modeled by the existing computational techniques. Since certain environmental conditions cannot be handled with the computational techniques presently in use, an attempt is being made to determine the need for, or importance of, further refinements in the propagation models.

The VLF propagation model initially incorporated into the propagation studies at the Corona Annex was the Wave Hop theory developed by L. A. Berry of the Environmental Science Services Administration (ESSA) (Ref. 3). This model was chosen initially because it was readily available in the form of a FORTRAN language digital computer program referred to as WAVEHOP (Ref. 4). Results obtained at the Corona Annex for the VLF propagation environment using this model have been documented in Ref. 5, 6, 7, and 8.

Under certain propagation conditions major inaccuracies exist in the generally available WAVEHOP computer program (see Ref. 4). The WAVEHOP program presently being used at Corona has been modified to correct for these deficiencies. A discussion to demonstrate the importance of these corrections is presented in the Appendix.

One of the inputs to the propagation model for predicting the VLF signal strength as a function of propagation range is an electron-density profile of the ionosphere. The "best-fit" profiles obtained in matching experimental sounder data for a variety of environmental conditions for daytime and nighttime propagation are discussed in the previously referenced Corona Annex publications.

It is of interest to compare the field-strength levels computed by WAVEHOP to those predicted by VLF propagation models developed at other organizations. A second computerized propagation model (see Ref. 9), based on waveguide mode theory and developed at the Naval Electronics Laboratory Center (NELC), San Diego, has been adapted to the Corona Annex computer, an IBM 360/50, to make theoretical calculations of VLF fields.

This report presents a comparison of the electric field strengths predicted by the ESSA WAVEHOP and the NELC WAVEGUIDE computer programs for the same set of environmental input conditions.

THE PROPAGATION MODELS

THE WAVE HOP MODEL

Of the several VLF radio propagation models described in the literature, most are based on waveguide mode theory. The Wave-Hop theory (see Ref. 3) provides full-wave solutions for the propagation of VLF radio waves between a homogeneous, spherical earth and an arbitrary, stratified ionosphere. This model is analytically and numerically equivalent to VLF mode theory, but the concepts are asymptotically related to HF ray-hop theory or geometric optics. This model decomposes the mode solutions into more geometrically meaningful components referred to as wave hops. The field at some distant point is considered to be the sum of the individual rays or hops, such as the direct or ground wave, plus the ray that has been reflected once from the ionosphere, plus the ray that has been reflected twice from the ionosphere and once from the ground, and so on.

Since the different rays will arrive at the receiver at different times because of the different lengths of the paths they have traveled, they are sometimes called time-modes to indicate this separation in time.

It is important to point out that the formulas used to compute the wave hops can be derived rigorously from the same complex propagation integral as found in the usual waveguide mode theories. The individual wave hops are computed taking into account the effects of diffraction and surface wave propagation.

The actual computer program for computing the radial electric fields using the Wave-Hop model consists of two parts, TUIK and WAVEHOP (see Ref. 4). The first part, TUIK, calculates the ionospheric reflection coefficients of an arbitrary stratified ionosphere as a function of the angle of the wave hop on the ionosphere, the propagation frequency, the magnitude and dip angle of the earth's magnetic field, the magnetic direction of propagation, a collision frequency profile, and an electron-density profile. The WAVEHOP program computes the vertical electric field at the receiver as the vector sum of individual hops and the ground wave. The inputs to WAVEHOP are the ionospheric reflection coefficients from TUIK, the propagation frequency, ground conductivity, relative dielectric constant of the earth, the propagation range, and the effective ionospheric reflection height.

THE WAVEGUIDE MODE MODEL

The waveguide mode theory as developed at NELC (see Ref. 10, 11, and 12) obtains the full-wave modal solution for a waveguide whose upper boundary has an arbitrary electron density distribution with height and whose lower boundary is a smooth homogeneous earth. In this theory, the electromagnetic waves are considered to propagate between the earth and the ionosphere as normal modes, analogous to microwave propagation in a lossy waveguide.

The modal equation for propagation within the earth ionosphere waveguide is solved for as many modes as desired. The eigenvalues (or eigenangles) so obtained are then used in a modal summation to compute the total field at some distant point from the transmitter. The effects of earth curvature are included in the calculation. The eigenangles are the angles of incidence at the height where the modified index of refraction becomes unity. The radial electric field is computed as a function of the earth's magnetic field parameters, a collision frequency profile, an electron density profile, propagation frequency, and the relative dielectric constant and conductivity at the earth over the propagation path.

The computer program developed around this mode theory is documented in Ref. 9. The computer program will be referred to as WAVEGUIDE.

PROGRAM COMPUTATIONS

Among the input parameters to these computerized propagation models is an electron density profile of the ionosphere. The profiles chosen for these comparisons are the exponential distributions described in Ref. 13. These profiles were chosen as they are the most commonly referenced in the literature for theoretical calculations of VLF propagation. The values of electron density N(Z) as a function of height Z, in kilometers, are calculated from the equation

$$N(Z) = N_o \exp(\beta - 0.15)Z - \beta h' + 0.15(70)$$

where

$$\beta = 0.5 \text{ km}^{-1}$$

$$N_o = 393 \text{ electrons/cm}^3$$

$$h' = 70,\ 75,\ 80,\ 85,\ \text{and } 90 \text{ km}$$

where $h' = 70$ km corresponds to the ambient daytime profile and $h' = 90$ km to the ambient nighttime profile. Figure 1 shows the height versus electron density relationship for the profiles $\beta = 0.5$ km^{-1}, $h' = 70$ km, $h' = 75$ km, $h' = 80$ km, $h' = 85$ km, and $h' = 90$ km.

The propagation path chosen for this comparison was that used for experimental work at Corona Annex. A transmitter station is located on the island of Hawaii (155.60°W, 19.642°N) with a propagation path passing through receiver coordinates in Southern California (116.625°W, 34.533°N), with a path length of about 4.2 megameters. The path is considered to be entirely over sea water.

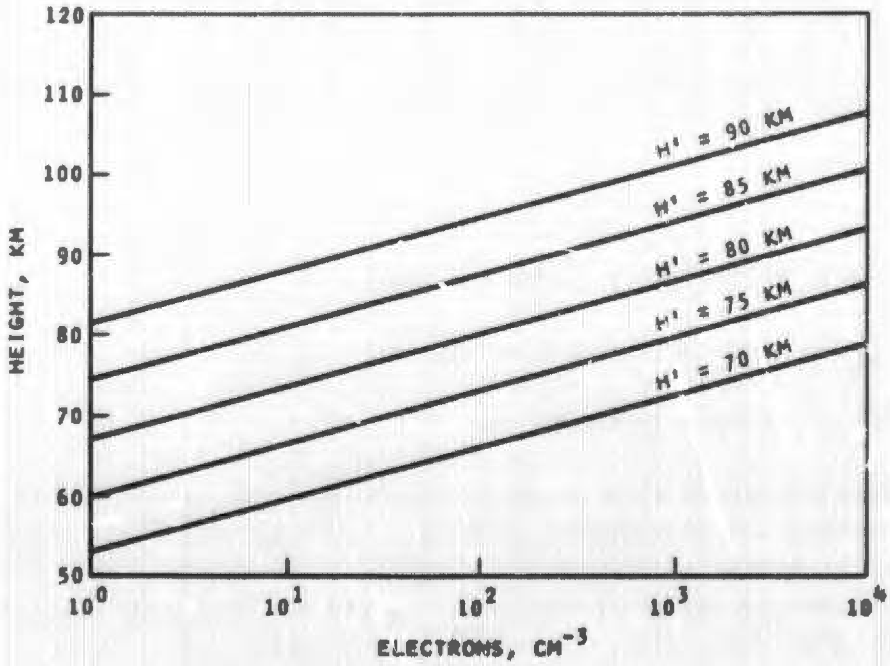

FIG. 1. Electron Density Profiles for a Conductivity Parameter of $\beta = 0.5\ km^{-1}$.

As described in Ref. 13 the collision frequency was chosen to be

$$\nu = \nu_o \exp(-\alpha Z)$$

where

$$\nu_o = 1.82 \times 10^{11} \text{ collisions/sec}$$

$$\alpha = 1.5 \times 10^{-4} \text{meters}^{-1}$$

$$Z = \text{meters}$$

The sea water propagation path parameters were permittivity and conductivity. The permittivity is

$$\epsilon = 7.172015 \times 10^{-10} \quad \frac{\text{farads}}{\text{meter}}$$

$$\epsilon_o = 8.85434 \times 10^{-12} \quad \frac{\text{farads}}{\text{meter}}$$

or

$$\epsilon_r = \frac{\epsilon}{\epsilon_o} = 81$$

where

ϵ = permittivity of the medium

ϵ_o = permittivity of free space

ϵ_r = relative permittivity

Conductivity is given as $\sigma = 5.0$ mhos/meter. The propagation path used for these computations may be assumed to be a horizontally homogeneous waveguide, and thus the earth's magnetic-field parameters along the propagation path may be assigned the values at midpath (see Ref. 14). The magnetic parameters at mid path were

$|H_e| = 4.25 \times 10^{-5}$ webers/meter^2

Dip = 50 deg (WAVEHOP)

Co-Dip = 40 deg (WAVEGUIDE)

Magnetic azimuth = 50.633 deg

Propagation frequencies were 15.567 kHz and 28.125 kHz.

The angles of incidence used in TUIK consisted of a range from 41 deg to 82 deg. The increment between these angles was chosen so that the phases of the ionospheric reflection coefficients obtained would be close enough to insure a smooth curve (no discontinuities because of ±180 deg changes). Interpolation is used to determine the reflection coefficient phases at the particular geometrical incidence angles of each hop on the propagation path; therefore, a continuous phase is mandatory.

The determination of the effective ionospheric reflection height used in WAVEHOP is based on the assumption that the upgoing field will be a maximum when it enters the ionosphere. The field should then decrease with height due to reflection and absorption, until a value approximately 10 dB below the original field level remains. The height so obtained is taken as the effective reflection height. This height also corresponds to a level about one-skin depth above the height where the rate of reflection of the incident wave maximizes. The most important reflection of the wave occurs within an altitude range of several kilometers centered at or near the height of maximum reflection, as discussed by Field and Engle (see Ref. 15), and the actual choice of the reflection height to be an input to WAVEHOP may vary over a few kilometers without significantly affecting the output field strength. For long VLF propagation paths, the angle of incidence is about 82 deg for the most important hops, and the reflection height which was determined for this angle was used in the computations. The WAVEHOP program was implemented using the values as shown in Tables 1 and 2.

TABLE 1. Frequency and Reflection Height Parameters Used in WAVEHOP Computations.

Profile	Frequency, kHz	Reflection height, km
β = 0.5 km^{-1}, h' = 70 km	15.567 28.125	66.6 68.2
β = 0.5 km^{-1}, h' = 75 km	15.567 28.125	72.8 73.5
β = 0.5 km^{-1}, h' = 80 km	15.567 28.125	79.4 80.6
β = 0.5 km^{-1}, h' = 85 km	15.567 28.125	86.3 88.1
β = 0.5 km^{-1}, h' = 90 km	15.567 28.125	94.0 95.4

The choice of reflection height values shown in Table 1 is not too critical in that the field strength values computed using reflection heights of 65 km ±5 km for the profile β = 0.5 km^{-1}, h' = 70 km were found to be nearly equal. Also, for the profile β = 0.5 km^{-1}, h' = 90 km profile, the values of the computed fields were found to be nearly equal for a reflection height of 95 km ±5 km. The WAVEGUIDE program was implemented using the values shown in Table 3.

TABLE 2. Distance and Number of Hops Used in WAVEHOP Computations.

Profile	Distance, km	No. of hops
β = 0.5 km^{-1}, h' = 70 km	1000-2000	5
	2000-3000	6
	3000-8000	9
β = 0.5 km^{-1}, h' = 75 km	1000-2000	5
	2000-3000	6
	3000-8000	9
β = 0.5 km^{-1}, h' = 80 km	1000-2000	5
	2000-3000	6
	3000-8000	9
β = 0.5 km^{-1}, h' = 85 km	1000-2000	5
	2000-3000	7
	4000-8000	9
β = 0.5 km^{-1}, h' = 90 km	1000-2000	5
	2000-4000	7
	4000-8000	10

TABLE 3. Height Parameters Used in WAVEGUIDE Computations.

Profile	D,[a] km	H,[b] km	REFLHT,[c] km
β = 0.5 km^{-1}, h' = 70 km	30	70	70
β = 0.5 km^{-1}, h' = 75 km	40	75	75
β = 0.5 km^{-1}, h' = 80 km	50	80	80
β = 0.5 km^{-1}, h' = 85 km	50	85	85
β = 0.5 km^{-1}, h' = 90 km	50	90	90

[a] D = The height below which ionospheric effects can be considered negligible relative to earth-curvature effects.

[b] H = The height which represents physically the height at which the modified refractive index becomes unity. This is the height at which the eigenangles are measured.

[c] REFLHT = The height chosen to be a reasonable estimate of where reflection occurs.

From the standpoint of program running time, it is desirable to choose D as large as possible since this minimizes the time involved in integrating the modal equation through the ionosphere. This computation is the most time consuming part of the WAVEGUIDE program. Care must be exercised to insure that the value of D be chosen low enough that the eigenvalue (eigenangle) solutions have stabilized (see Ref. 10).

The values of D, H, and REFLHT presented in Table 3 need not be precise, because different values may be used to obtain the same field strength values. For example, four sets of values for D, H, and REFLHT were used with the β = 0.5 km^{-1}, h' = 70 km profile from which identical field strengths resulted. The four sets of kilometer values for D, H, and REFLHT were, respectively, 30, 50, 70; 50, 50, 70; 30, 50, 65; and 50, 50, 65.

A similar investigation was made for the β = 0.5 km^{-1}, h' = 85 km profile. The values used for computing field strengths were 30, 85, 85 km; 50, 50, 85 km; and 50, 50, 90 km, for D, H, and REFLHT, respectively. Again identical field strength results were obtained.

Summaries of the parameters obtained from the WAVEGUIDE computations are found in Tables 4 through 13 for the five electron-density profiles at the two frequencies shown. In these tables, the real and imaginary parts of the eigenangles of the various modes are listed under Theta. As shown in the tables, when the real part of Theta increases, the imaginary part generally increases in value. The ratio of phase velocity in the medium to that in free space is V/C. The ratio V/C is seen to decrease with increasing real eigenangle, indicating a decreasing phase velocity or increasing refractive index. The importance of a given mode is determined by the attenuation and excitation factors. The most dominant mode is described by a low attenuation value and a large positive excitation value. The tables illustrate that the attenuation(dB/megameter)decreases with increasing real angle of incidence. The Polarization Magnitude term is a measure of the extent of polarization mixing (see Ref. 12). Values of this parameter which are much greater than unity indicate a nearly pure TM mode (vertical polarization) while values much less than unity indicate a pure TE mode (horizontal polarization). Values of the ratio close to unity indicate that a nearly equal mixture of TE and TM components comprise the mode. The tables indicate that for these frequencies, the modes which are quasi-TM are more important in the mode sum than those which are quasi-TE, in that the quasi-TM modes are more highly excited. A convenient rule of thumb in insuring that all modes are being used in the computation for the fields is that the polarisation term should alternate between values greater than one and less than one. This relationship is illustrated in Tables 4 through 13. Table 9 does not follow the relationship at 82.661 deg and 82.890 deg. This would indicate that a mode was missed with a real eigenangle between these two values. It was not possible, however, to find such an eigenvalue. The computations of Table 11 indicate a similar problem between 80.812 deg and 82.654 deg, while Table 13 shows that this occurs between 80.874 deg and 82.658 deg. This could be explained as follows: some eigenangles, particularly at 89 deg, have small attenuation rates but also very small excitation factors and consequently have little effect on the total electric field strength value. These are called "earth-detached" modes, (see Ref. 16). The foregoing eigenangles, in particular 82.661 deg and 82.890 deg from Table 9, 82.654 deg from Table 11, and 82.658 deg from Table 13, may also be considered earth-detached and as such their behavior in the polarization magnitude scheme might be explained.

TABLE 4. Summary of WAVEGUIDE Parameters at 15.567 kHz for $\beta = 0.5\ km^{-1}$, $h' = 70$ km.

Theta, deg		V/C	Attenuation, dB/mega-meter	Excitation factor, dB	Polarization	
Real	Imaginary				Magnitude	Angle, deg
64.290	-1.249	1.097415	27.099319	-35.69444	0.187769	13.49584
67.608	-1.015	1.069492	19.337585	-0.28066	12.217490	52.68211
72.480	-0.794	1.037018	11.953999	-42.66788	0.115792	9.64833
75.773	-0.572	1.020250	7.030396	0.76325	17.611496	52.02216
79.862	-0.404	1.004669	3.556337	-49.89520	0.062235	30.23956
81.724	-0.172	0.999412	1.238154	-1.63192	32.158966	88.96785
89.990	0.003	0.989008	-0.000026	-137.49515	0.005799	115.18188

TABLE 5. Summary of Waveguide Parameters at 28.125 kHz for $\beta = 0.5\ km^{-1}$, $h' = 70$ km.

Theta, deg		V/C	Attenuation, dB/megameter	Excitation factor, dB	Polarization	
Real	Imaginary				Magnitude	Angle, deg
67.999	-0.863	1.066565	29.212234	-0.46685	5.925715	69.64754
70.633	-0.916	1.048195	27.447037	-34.53508	0.133177	1.01856
72.526	-0.671	1.036783	18.205078	0.12703	7.313920	69.01436
74.940	-0.679	1.024112	15.940947	-39.95148	0.094010	7.09345
76.786	-0.476	1.015871	9.831292	0.97377	12.164526	75.22852
78.950	-0.449	1.007658	7.775711	-45.59265	0.062676	358.64966
80.447	-0.258	1.002905	3.868734	2.24449	14.374891	90.04794
82.494	-0.289	0.997543	3.411057	-42.45749	0.122350	47.44543
82.778	-0.155	0.996914	1.760603	-7.72704	6.429727	169.88083
89.980	0.001	0.989008	-0.000032	-137.14377	0.0	89.99997

TABLE 6. Summary of Waveguide Parameters at 15.567 kHz for $\beta = 0.5\ km^{-1}$, h' = 75 km.

Theta, deg		V/C	Attenuation, dB/mega-meter	Excitation factor, dB	Polarization	
Real	Imaginary				Magnitude	Angle, deg
66.215	-1.042	1.079768	21.034241	-28.53926	0.239821	2.63871
69.196	-0.674	1.057074	11.981479	-0.16209	6.773071	68.17528
73.624	-0.665	1.029938	9.384047	-35.26738	0.160650	3.26129
76.546	-0.392	1.016083	4.564807	0.88612	11.006417	64.01772
80.268	-0.350	1.002632	2.961166	-40.94304	0.087120	22.19275
81.706	-0.125	0.998666	0.902479	-2.42902	15.877316	128.70358
89.988	0.002	0.988222	-0.000021	-141.37369	0.008398	115.13184

TABLE 7. Summary of Waveguide Parameters at 28.125 kHz for $\beta = 0.5\ km^{-1}$, h' = 75 km.

Theta, deg		V/C	Attenuation, dB/mega-meter	Excitation factor, dB	Polarization	
Real	Imaginary				Magnitude	Angle, deg
67.989	-0.906	1.065782	30.705536	-21.08469	0.280973	336.80908
69.526	-0.616	1.054795	19.483932	-0.45940	3.009709	69.35957
72.042	-0.731	1.038746	20.380737	-25.64145	0.205898	338.16431
73.623	-0.494	1.029974	12.595168	0.21603	4.116412	70.10898
75.904	-0.555	1.018853	12.222857	-30.65016	0.129614	338.09302
77.452	-0.359	1.012383	7.052810	1.19597	5.608160	78.65514
79.460	-0.377	1.005159	6.235909	-34.58418	0.104922	338.43628
80.623	-0.188	1.001600	2.769808	2.21072	7.220531	84.08716
82.620	-0.279	0.996465	3.240633	-29.94334	0.306434	8.13619
82.764	-0.140	0.996152	1.594564	-12.54633	1.853441	206.61401

TABLE 8. Summary of Waveguide Parameters at 15.567 kHz for $\beta = 0.5\ km^{-1}$, $h' = 80$ km.

Theta, deg		V/C	Attenuation, dB/mega-meter	Excitation factor, dB	Polarization	
Real	Imaginary				Magnitude	Angle, deg
63.293	-0.577	1.105305	12.989402	-1.36378	3.129542	80.29333
67.865	-0.821	1.065894	15.495461	-23.01541	0.310205	344.79517
70.615	-0.442	1.046748	7.348512	-0.24807	4.407783	76.61931
74.609	-0.516	1.024125	6.859793	-29.19182	0.205012	348.31396
77.214	-0.266	1.012533	2.948713	0.98845	7.614028	76.52620
80.611	-0.285	1.000833	2.328875	-33.13902	0.128496	8.11715
81.686	-0.087	0.997924	0.630129	-3.48685	6.653981	141.95859
89.991	-0.003	0.987438	0.000024	-153.57190	0.017737	344.88843

TABLE 9. Summary of Waveguide Parameters at 28.125 kHz for $\beta = 0.5\ km^{-1}$, h' = 80 km.

Theta, deg		V/C	Attenuation, dB/megameter	Excitation factor, dB	Polarization	
Real	Imaginary				Magnitude	Angle, deg
67.036	-0.467	1.072392	16.488831	-2.15791	1.708636	65.26321
69.525	-0.607	1.053967	19.215393	-13.62779	0.513407	316.42432
70.898	-0.418	1.044949	12.379257	-1.10132	2.108592	64.07761
73.229	-0.482	1.031266	12.586476	-17.26471	0.359327	315.85596
74.598	-0.348	1.024201	8.364258	-0.06498	2.722632	70.19466
76.723	-0.368	1.014533	7.648388	-21.23329	0.259620	310.16772
78.026	-0.257	1.009390	4.825250	1.27671	3.200137	73.46654
79.888	-0.259	1.003008	4.115238	-23.65295	0.219967	320.79077
80.740	-0.127	1.000473	1.849419	1.65285	4.279541	91.19252
82.661	-0.227	0.995587	2.624161	-22.67204	0.905500	346.35791
82.890	-0.122	0.995087	1.366551	-24.83273	0.727605	204.11745

TABLE 10. Summary of Waveguide Parameters at 15.567 kHz for $\beta = 0.5\ km^{-1}$, $h' = 85$ km.

Theta, deg		V/C	Attenuation, dB/megameter	Excitation factor, dB	Polarization	
Real	Imaginary				Magnitude	Angle, deg
62.509	-0.960	1.112085	22.215591	-14.60308	0.577910	329.73120
65.242	-0.403	1.086492	8.460461	-2.01493	2.605300	84.24753
69.238	-0.628	1.055109	11.159905	-18.85110	0.403090	326.81079
71.845	-0.316	1.038326	4.935863	-0.52766	3.408094	84.65630
75.420	-0.384	1.019459	4.845797	-24.24103	0.289466	329.55957
77.767	-0.191	1.009568	2.028769	0.96218	5.466550	80.95462
80.869	-0.230	0.999307	1.829692	-25.84442	0.221352	2.02758
81.678	-0.058	0.997151	0.420824	-5.09335	4.040819	155.89731

TABLE 11. Summary of Waveguide Parameters at 28.125 kHz for $\beta = 0.5\ km^{-1}$, h' = 85 km.

Theta, deg		V/C	Attenuation, dB/mega-meter	Excitation factor, dB	Polarization	
Real	Imaginary				Magnitude	Anglc, deg
67.211	-0.520	1.070148	18.242294	-6.99214	0.992478	306.76660
68.576	-0.344	1.059868	11.380239	-4.00963	1.382699	63.15662
70.785	-0.405	1.044834	12.072172	-9.13138	0.770695	302.56445
72.077	-0.306	1.036959	8.528738	-2.30005	1.570908	63.54758
74.184	-0.308	1.025458	7.602866	-11.95107	0.584410	305.66626
75.425	-0.256	1.019449	5.834623	-0.71824	2.159298	66.22102
77.361	-0.227	1.011146	4.498512	-14.86057	0.388796	300.64893
78.492	-0.184	1.006887	3.324704	1.20421	2.423215	79.39552
80.186	-0.169	1.001299	2.608955	-15.02133	0.411545	309.40625
80.81[illegible]	-0.077	0.999474	1.113542	0.01832	2.167155	101.62277
82.654	-0.204	0.994811	2.362394	-25.89392	1.344164	353.85425
83.067	-0.065	0.993918	0.710613	-37.15074	0.658765	190.38757

TABLE 12. Summary of Waveguide Parameters at 15.567 kHz for β = 0.5 km^{-1}, h' = 90 km.

Theta, deg		V/C	Attenuation, dB/megameter	Excitation factor, dB	Polarization	
Real	Imaginary				Magnitude	Angle, deg
60.472	-0.376	1.133006	9.296992	-5.06141	1.702432	87.11026
64.212	-0.709	1.094825	15.474374	-12.09672	0.753823	314.26318
66.896	-0.322	1.071816	6.339072	-2.81639	2.323418	88.29460
70.423	-0.463	1.046321	7.783310	-15.83295	0.502564	311.98071
72.876	-0.251	1.031588	3.707755	-0.91193	2.964911	89.46432
76.102	-0.283	1.015586	3.410278	-20.57822	0.385714	312.08350
78.205	-0.147	1.007128	1.507507	0.90061	4.239605	84.27917
81.053	-0.191	0.998004	1.490262	-20.28026	0.394766	357.58643
81.695	-0.038	0.996315	0.275371	-7.80828	2.620982	166.78784
89.989	0.003	0.985867	-0.000029	-153.39684	0.031168	3.41930

TABLE 13. Summary of Waveguide Parameters at 28.125 kHz for $\beta = 0.5\ km^{-1}$, h' = 90 km.

Theta, deg		V/C	Attenuation, dB/mega-meter	Excitation factor, dB	Polarization	
Real	Imaginary				Magnitude	Angle, deg
61.560	-0.509	1.121130	21.972153	-2.85852	2.444879	303.43652
63.142	-0.341	1.105053	13.964008	-11.82327	0.813592	47.13593
65.147	-0.433	1.086455	16.495590	-3.51609	1.778311	298.00513
66.554	-0.299	1.074574	10.783415	-8.96648	0.866296	54.23936
68.586	-0.356	1.058949	11.781331	-4.74999	1.371325	298.36230
69.862	-0.268	1.050049	8.363271	-6.33167	1.076632	58.66864
71.876	-0.276	1.037321	7.782177	-6.46030	0.962279	294.50171
73.060	-0.237	1.030573	6.259215	-3.90550	1.225620	66.90196
74.994	-0.206	1.020666	4.834593	-8.70418	0.809712	294.94971
76.106	-0.198	1.015574	4.309546	-1.69150	1.634636	63.95689
77.880	-0.148	1.008339	2.816595	-10.86768	0.507472	300.27026
78.853	-0.137	1.004819	2.400707	0.78766	2.146343	85.72569
80.382	-0.127	0.999920	1.923321	-9.27415	0.578400	308.43750
80.874	-0.039	0.998506	0.560677	-3.90118	1.166057	126.94872
82.658	-0.186	0.994012	2.154495	-31.03848	1.505057	358.31055
83.237	-0.028	0.992775	0.298878	-47.32495	0.648848	184.53349
89.987	0.004	0.985866	-0.000083	-176.49695	0.007158	16.00693

Examples illustrating the relative field-strength magnitudes for the individual waveguide mode components and the wave-hop components of the total field are presented in Fig. 2 and 3, respectively. These results are determined for the daytime ionospheric profile $\beta = 0.5\ km^{-1}$, h' = 70 km, at 28.125 kHz. It is shown in Fig. 2 that only three modes, all of which are of the quasi-TM type, are necessary to completely describe the propagated field for this case; and at ranges beyond about 4 megameters two modes are sufficient. Table 5 illustrates that many modes can be computed for this profile and propagation frequency, but only those modes with low attenuation rates and high excitation factors are important in comprising the total mode sum of the fields.

A similar breakdown of the wave-hop computation is shown in Fig. 3. For the range 1.0 to 8.0 megameters, it is observed that energy traveling by the way of the ground wave, and the one-hop path, two-hop path, and so on up to a seven-hop path, can be important in the total propagated field. The actual significance of any hop path depends on the particular range of interest. At 1 megameter only the groundwave, one-, two-, and three-hop paths are important. At a distance of 4 megameters the ground wave is completely negligible, but the four- and five-hop paths have become significant. At 6 megameters the one-hop path is no longer important, but the six-hop path must be included in the total field-strength computation. Beyond 8 megameters the two-hop path is no longer of value, but the seven-hop path must be included to obtain the total field.

In general, for the propagation ranges considered here, it may be inferred that for the waveguide model at least two but no more than three modes must be included in the computation for the total field strength levels for the daytime ionosphere. On the other hand, as many as five wave-hop components are needed to describe the same fields by the wavehop theory.

The waveguide mode and wave hop comparison for nighttime signal levels is illustrated in Fig. 4 and 5, respectively, for the profile $\beta = 0.5\ km^{-1}$, h' = 85 km at 28.125 kHz. It is observed for the waveguide model in Fig. 4 that as many as eight modes are important at 1.0 megameter for the nighttime condition, whereas for the daytime situation only three modes were significant. It is apparent, however, that most of these modes attenuate rapidly with distance so that beyond 5 megameters only four modes are really significant to the makeup of the total field level. An examination of Table 11 demonstrates that the

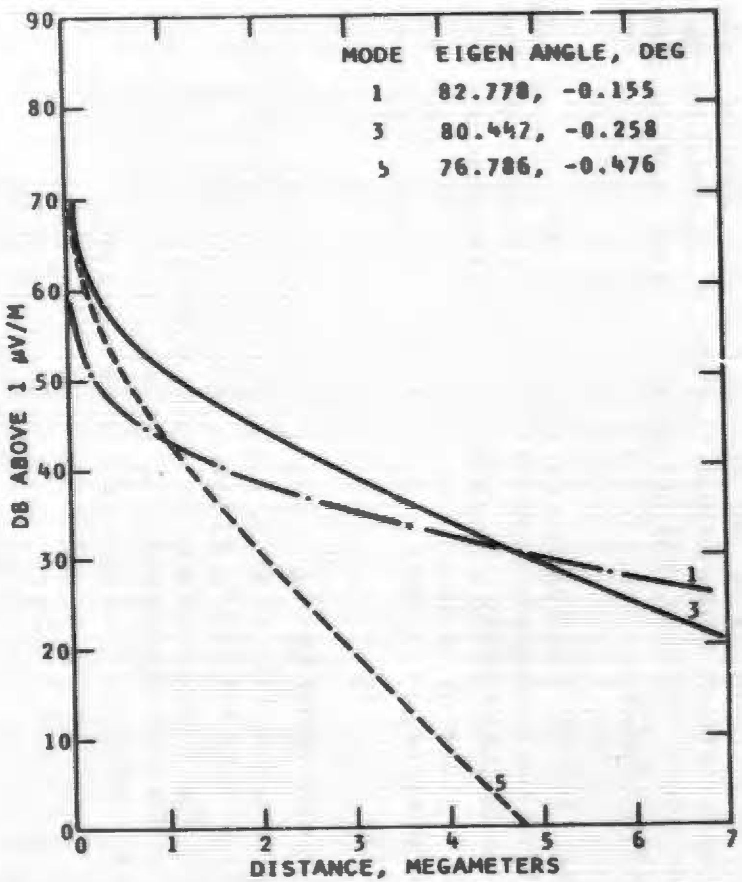

FIG. 2. Waveguide Mode Fields for Daytime Profile ($\beta = 0.5\ km^{-1}$, $h' = 70\ km$) at 28.125 kHz.

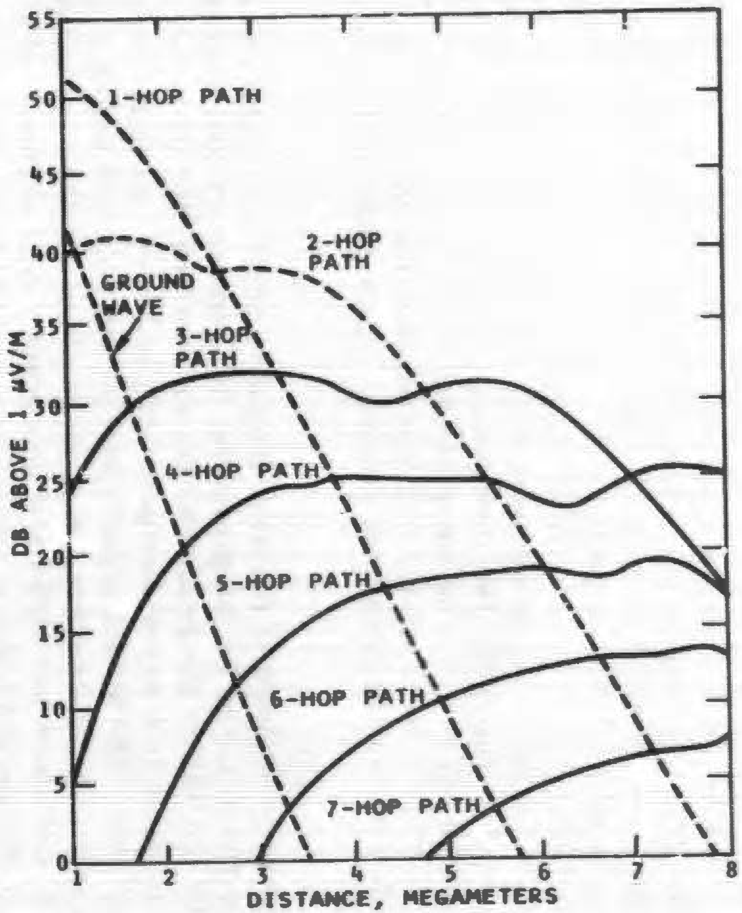

FIG. 3. Wavehop Fields for Daytime Profile ($\beta = 0.5\ km^{-1}$, $h' = 70\ km$) at 28.125 kHz.

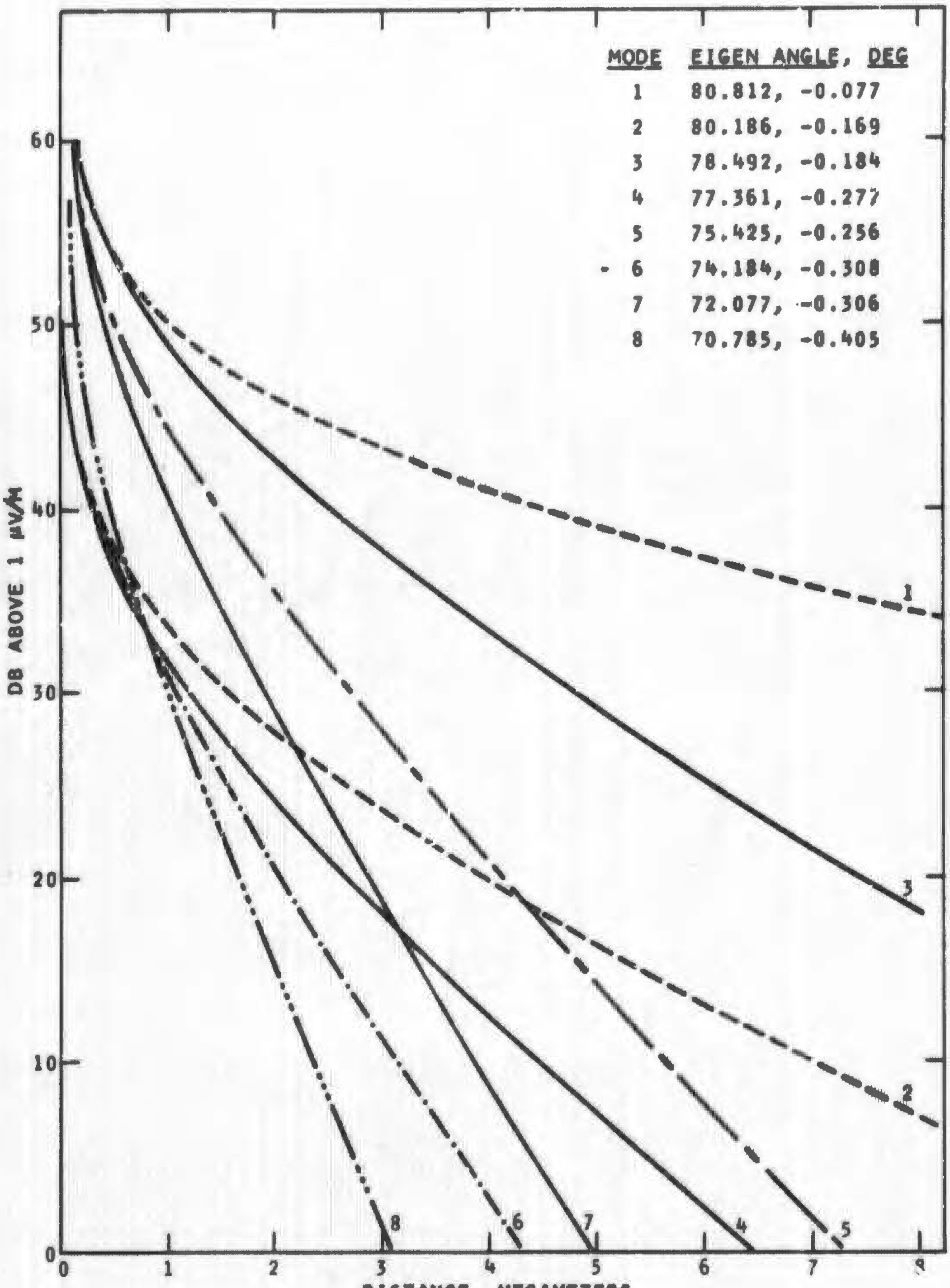

FIG. 4. Waveguide Mode Fields for Nighttime Profile (β = 0.5 km^{-1}, h' = 85 km) at 28.125 kHz.

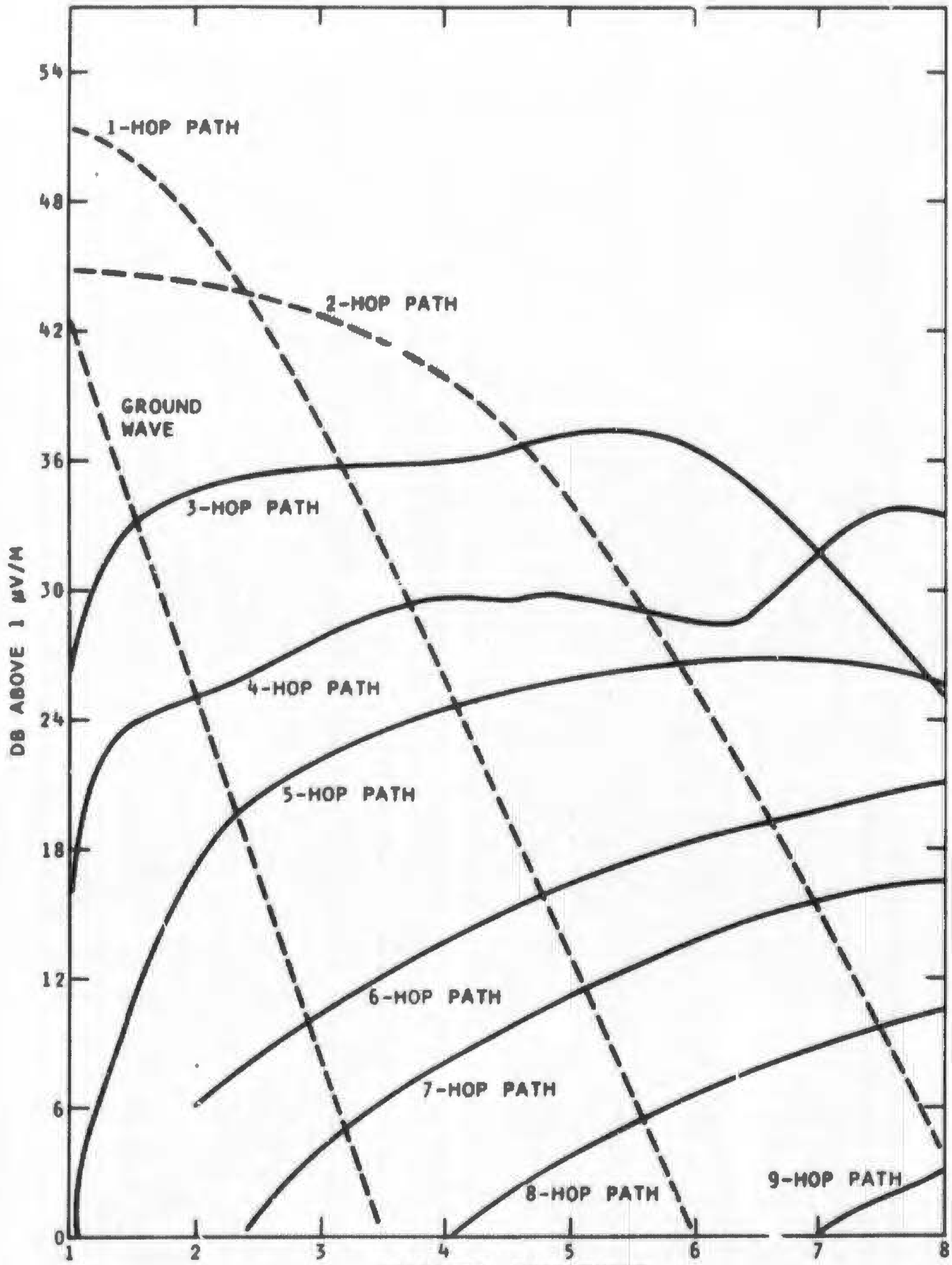

FIG. 5. Wavehop Fields for Nighttime Profile (β = 0.5 km^{-1}, h' = 85 km) at 28.125 kHz.

two most dominant modes (that is, No. 1 and 3 of Fig. 4) are not as purely quasi-TM as was found for the daytime condition of Table 5.

Figure 5 illustrates the wave-hop field components for the night-time case. It is observed here, as was demonstrated for the daytime situation, that several wave-hop paths must be considered when determining the total signal strength available at any given range. Comparison with the daytime results shows that, in general, a larger number of wave hops are important for nighttime propagation, where as many as seven wave-hop components are significant at 5 megameters. Also, where only four or less modes would be considered significant beyond 5 megameters, in the waveguide model, it is apparent from Fig. 5 that at least seven wave-hop components would need to be included in determining the total field for these ranges.

DISCUSSION OF RESULTS

The field-strength values computed from the WAVEHOP and the WAVEGUIDE computer programs, using the input parameters as described previously, are illustrated in Fig. 6 through 19 as a function of propagation range. The field-strength values were computed at 25-km intervals. The frequencies of propagation are 15.567 kHz and 28.125 kHz. The electron-density profiles are identified as $\beta = 0.5\ km^{-1}$, h' = 70, 75, 80, 85, and 90 km. The propagation path is entirely over sea water. The computed fields are normalized to 1 kW of radiated power at each frequency.

Figure 6 shows the comparison between the field strength values computed using WAVEHOP and WAVEGUIDE for the $\beta = 0.5\ km^{-1}$, h' = 70 km, (daytime) profile at 15.567 kHz. In general, the agreement between the two calculations appears to be good. The average attenuation rates of both signals are almost identical, and the amount of modal interference structure predicted is essentially the same for the two propagation models. This structure disappears, however, beyond 6 megameters, where the two computations differ by a maximum of 2 dB. At the 4.2 megameter distance, which is the length of the path used by the Corona Annex in obtaining VLF measurements, the value of the field strength computed using WAVEHOP is seen to be 1.5 dB higher than that obtained from WAVEGUIDE. The most noticeable discrepancy between the two curves is that the signal levels computed by WAVEHOP tend to occur at distances of about 150 to 200 km greater than where the same values of signal levels are computed by WAVEGUIDE. The actual value

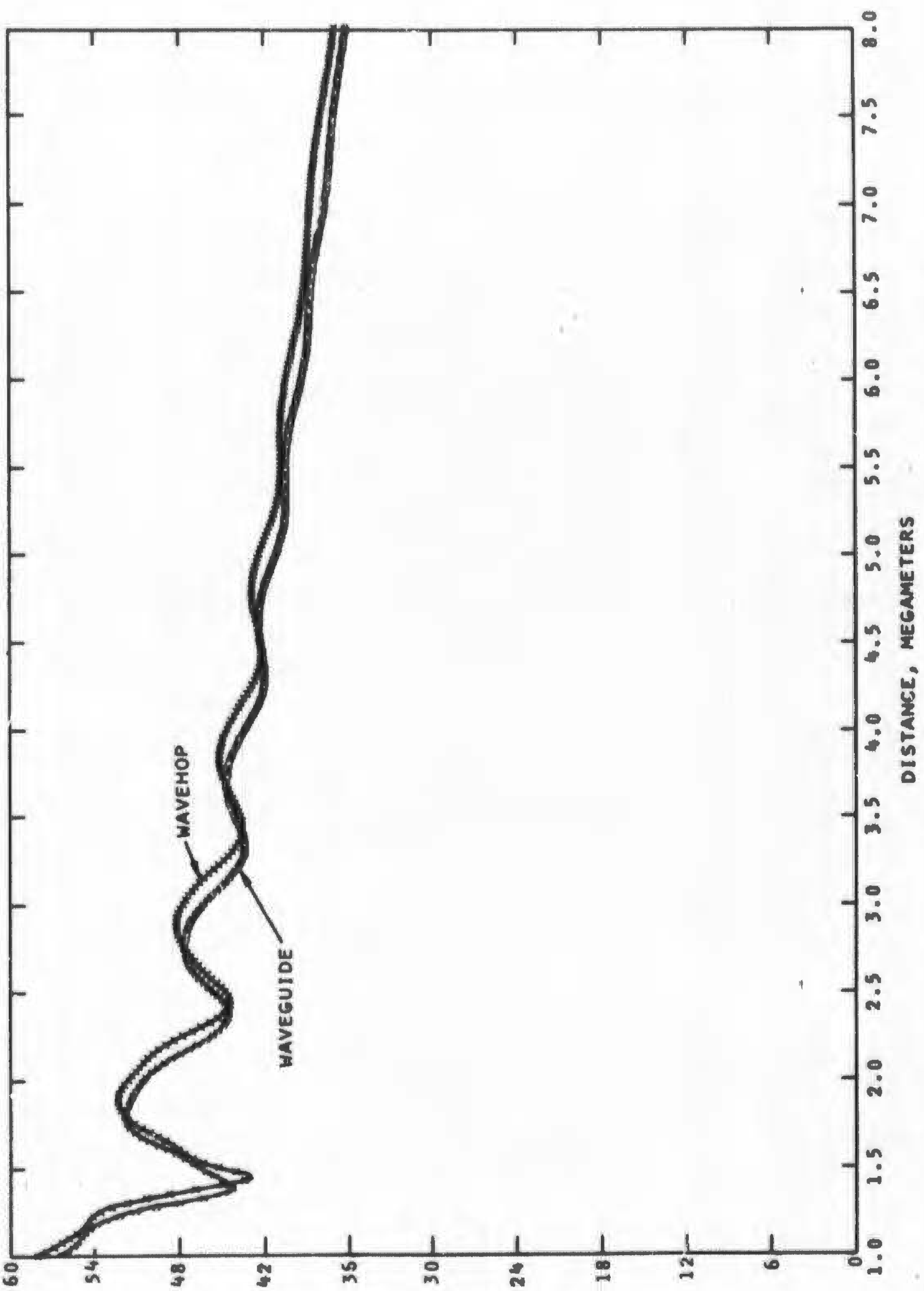

FIG. 6. Field Strength Versus Distance for WAVEHOP and WAVEGUIDE Comparison at 15.567 kHz (β = 0.5 km^{-1}, h' = 70 km).

of this difference interval varies with the propagation range, with the smallest discrepancy occurring closest to the transmitter.

Figure 7 illustrates the comparison between field strength levels for the profile $\beta = 0.5\ km^{-1}$, h' = 70 km, for a frequency of 28.125 kHz. It is of interest that the modal interference computed for this frequency is much greater than that found for 15.567 kHz. The agreement between the field strengths obtained by the two computational methods is fairly good, except in the vicinity of the signal nulls. These nulls are the result of destructive interference in the vector summation of the field hops (or modes). The nulls computed by WAVEHOP occur at a slightly greater range than the corresponding nulls computed by WAVEGUIDE. As for the 15.567-kHz fields, the values computed by WAVEHOP occur at approximately 150-to 200-km greater distances than do similar values computed by WAVEGUIDE. Also, the location of the null containing the deepest signal fade does not coincide for the two models. The deepest null found from the WAVEGUIDE computation is located at 4.50 megameters with a shallower null located at 6.25 megameters. The WAVEHOP computation, however, shows the shallower null at 4.75 megameters and the deeper null positioned at 6.50 megameters. At the 4.2 megameter distance the WAVEHOP signal level is computed to be 4.0 dB higher than that computed using WAVEGUIDE. For a receiver located at the 4.5-megameter distance, the two models yield signal levels which differ by as much as 20 dB.

In a first attempt to determine the reason for the differences in the field levels obtained for the two models, the ionosphere electron density profile used in the WAVEHOP program was lowered 1 km in height. This lowered profile was then input to the WAVEHOP program with the result as shown in Fig. 8. The signal-level nulls from this calculation are seen to line up much better (in range) with those determined from WAVEGUIDE. The relative depth of the signal nulls, however, continues to differ considerably. The observation that the WAVEGUIDE computation gives a field-strength level 15 dB below that of WAVEHOP for the signal null at 4.5 megameters and 15 dB above that of WAVEHOP for the null at 6.25 megameters indicates that fundamental differences do exist between the two propagation theories.

The comparisons of the field strength values computed using the profile $\beta = 0.5\ km^{-1}$, h' = 75 km for 15.567 kHz and 28.125 kHz are displayed in Fig. 9 and 10, respectively. The signal levels computed at 15.567 kHz by the two models are quite similar as a function of propagation distance. The average attenuation rates of the two field

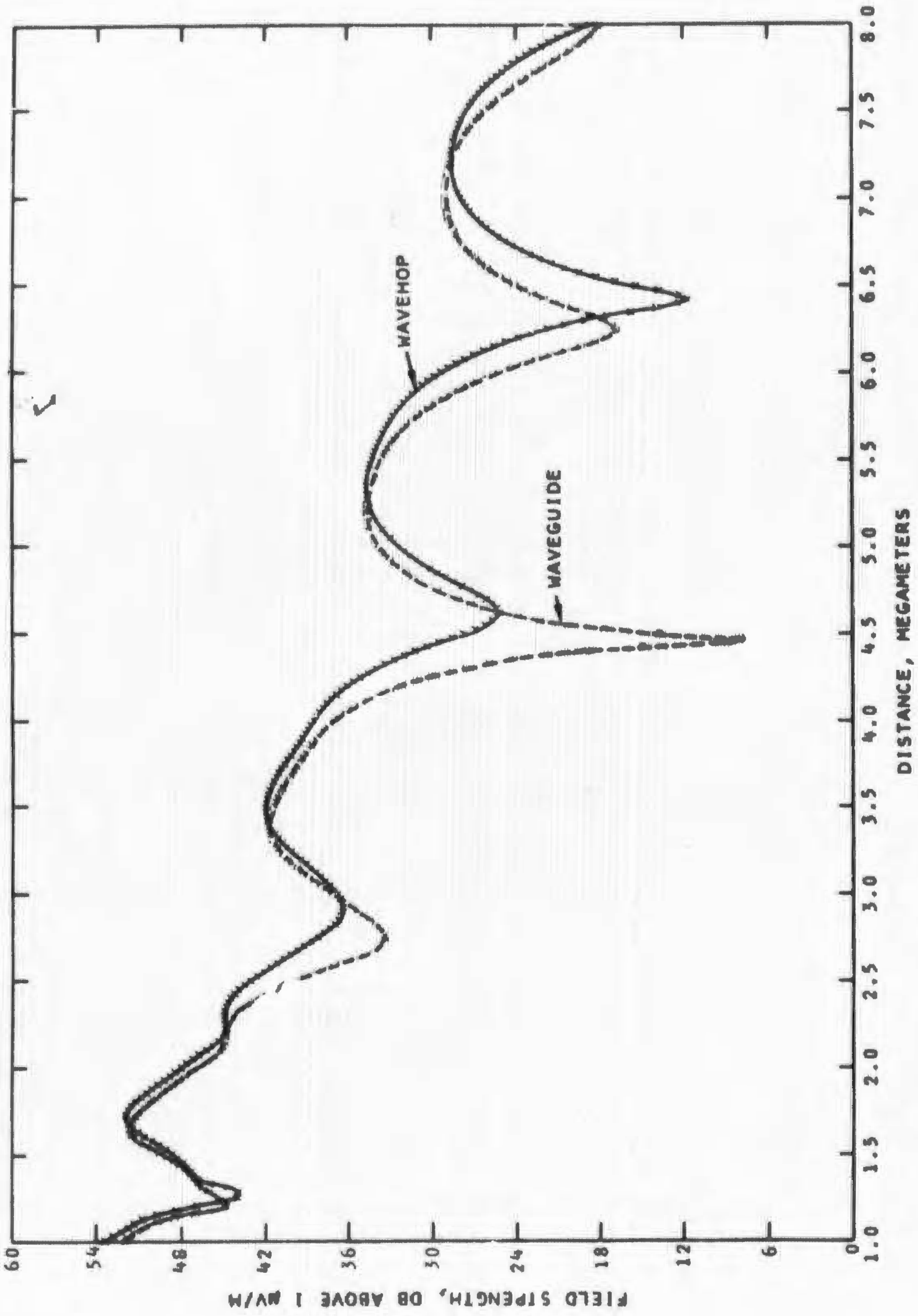

FIG. 7. Field Strength Versus Distance for WAVEHOP and WAVEGUIDE Comparison at 28.125 kHz ($\beta = 0.5\ km^{-1}$, $h' = 70$ km).

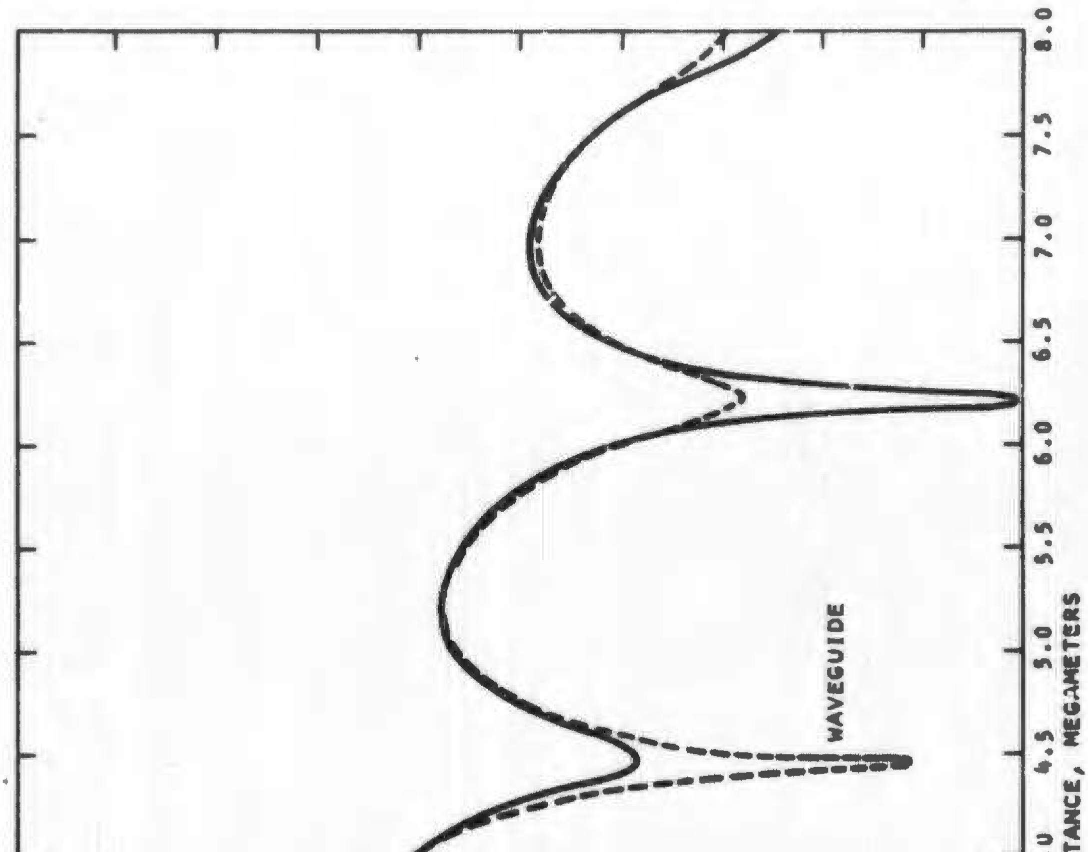

FIG. 8. Field Strength Versus Distance for WAVEHOP ($\beta = 0.5\ km^{-1}$, h' = 70 km - 1.0 km) - WAVEGUIDE ($\beta = 0.5\ km^{-1}$, h' = 70 km) Comparison at 28.125 kHz.

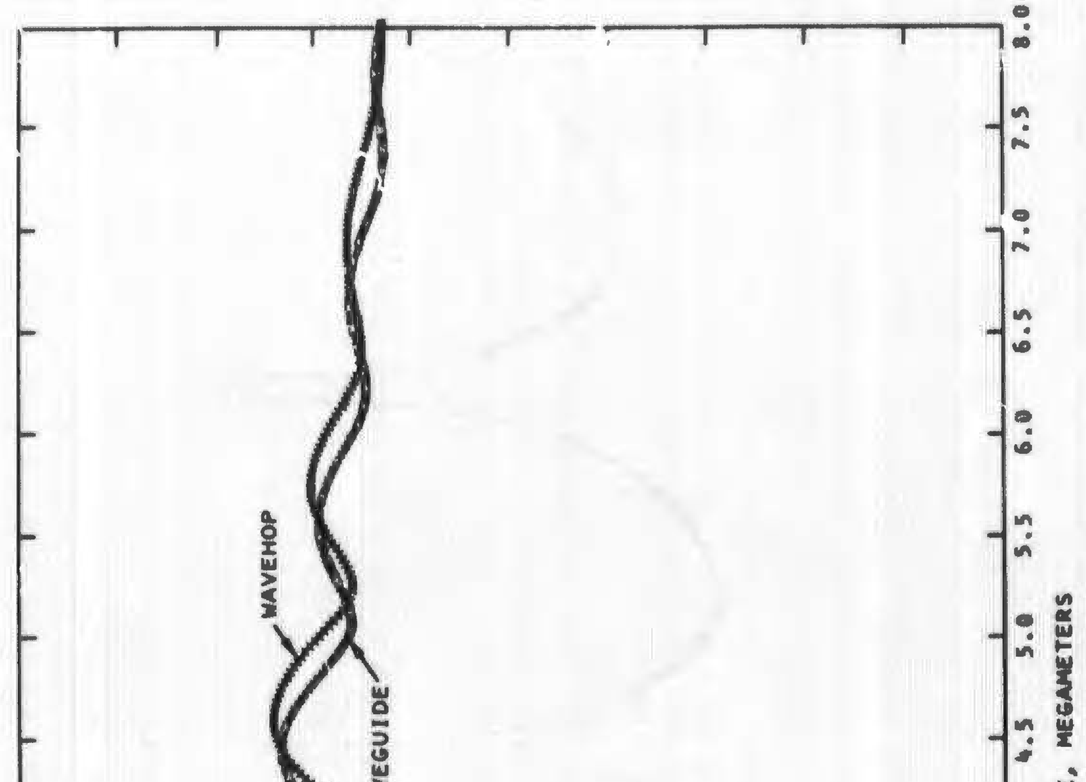

FIG. 9. Field Strength Versus Distance for WAVEHOP and WAVEGUIDE Comparison at 15.567 kHz ($\beta = 0.5\ km^{-1}$, $h' = 75$ km).

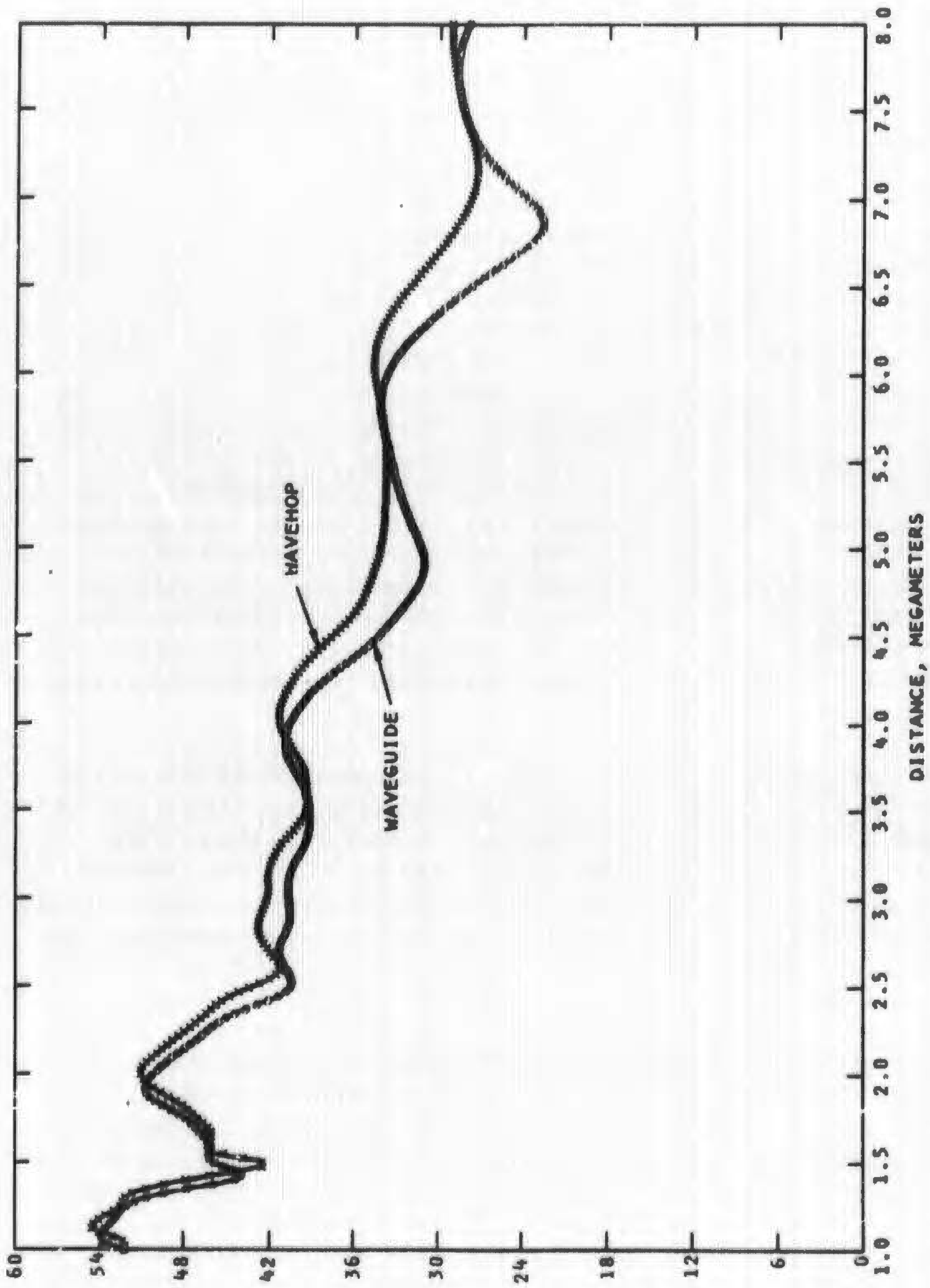

FIG. 10. Field Strength Versus Distance for WAVEHOP and WAVEGUIDE Comparison at 28.125 kHz (β = 0.5 km^{-1}, h' = 75 km).

curves appear to be essentially equal. Both calculations show deeper mode structures which increase to greater ranges than those found for the h' = 70 km profile at 15.567 kHz. A distance interval of 150 to 200 km exists between equal data values computed by the two methods for this profile as was found for the previous profile. At the 4.2-megameter distance the fields computed using the two models differ by 2 dB. There is also a difference of approximately 5 dB in the depth of the null computed by the two methods in the vicinity of 1.5 megameters. For the 28.125-kHz signal, the $\beta = 0.5\ km^{-1}$, h' = 75 km profile does not show as good an agreement between the signal levels computed by the two models as was determined for the cases so far considered. In general, WAVEHOP is seen to predict slightly higher signal levels beyond 4.0 megameters than WAVEGUIDE. The largest deviation between the two computations is 6 dB at 6.75 megameters, while at 4.2 megameters the difference is 2 dB. Again, the values computed by WAVEHOP tend to lead those of WAVEGUIDE by distance intervals ranging from 150 km at 1.5 megameters to 250 km at 6 megameters. A lowering of the electron-density profile as input to the WAVEHOP computation would tend to improve the comparison between the two programs, but the relative depth of the interference nulls which are characteristic of either model will remain unequal. This result is an indication of the presence of some dissimilarity in theory between the two propagation models.

The comparisons between the computed signal levels obtained for the profile $\beta = 0.5\ km^{-1}$, h' = 80 km are shown in Fig. 11 and 12. The patterns of field strength as a function of distance for the two frequencies are similar for the WAVEHOP and WAVEGUIDE methods. In fact, a shift inward of the WAVEHOP values would agree very well with the WAVEGUIDE results. The fields as now computed, however, can give large deviations between the two propagation models at a given distance. In particular, the discrepancy for 15.567 kHz (see Fig. 11) is 3.0 dB at 4.50, 5.0, 5.75, and 6.25 megameters; 2 dB at 4.2 megameters, and as much as 18 dB at 1.9 megameters. For 28.125 kHz (see Fig. 12) the discrepancy between the two models reaches 2 dB at several ranges. It is of interest that model interference structure is still prevalent as far out as 8.0 megameters in the fields computed for 15.567 kHz, whereas the existence of interference structure has essentially disappeared beyond 7 megameters for 28.125 kHz. This result may be contrasted to the daytime profile, $\beta = 0.5\ km^{-1}$, h' = 70 km, where considerable interference structure was found throughout the 8.0 megameter range at 28.125 kHz and very little interference structure was present beyond 5.5 megameters for 15.567 kHz.

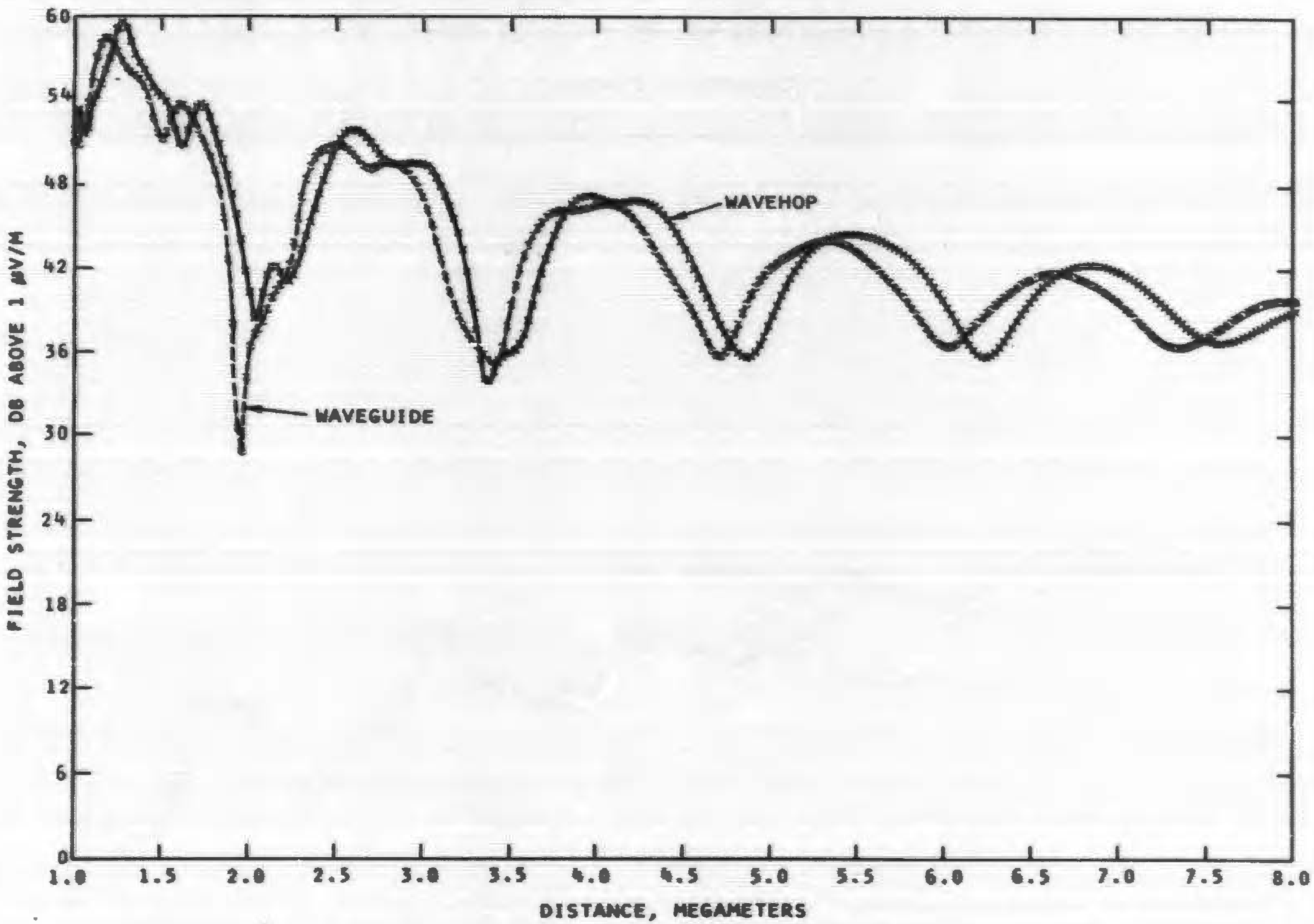

FIG. 11. Field Strength Versus Distance for WAVEHOP and WAVEGUIDE Comparison at 15.567 kHz (β = 0.5 km^{-1}, h' = 80 km).

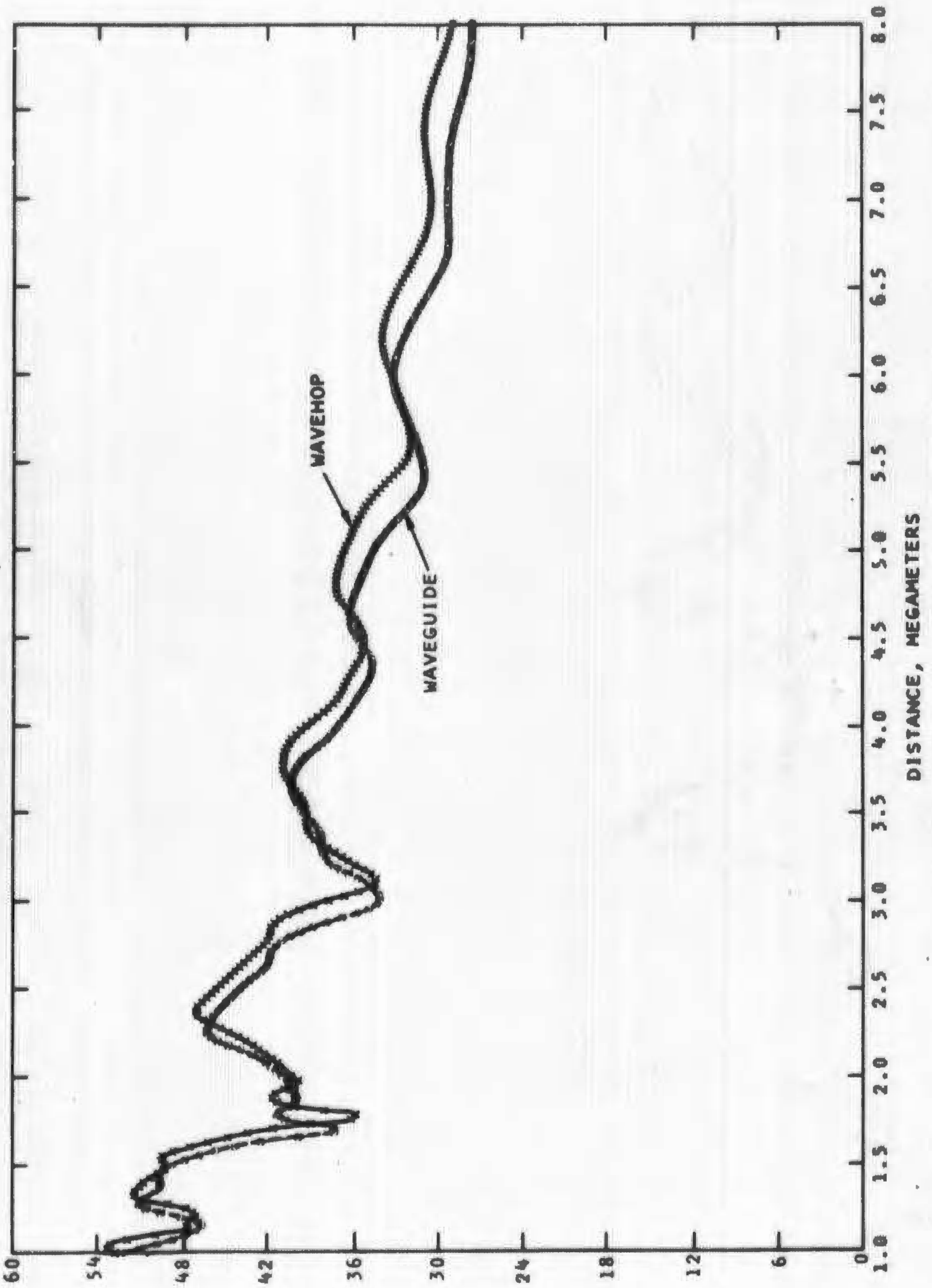

FIG. 12. Field Strength Versus Distance for WAVEHOP and WAVEGUIDE Comparison at 28.125 kHz ($\beta = 0.5$ km^{-1}, $h' = 80$ km).

Figure 13 illustrates the fields computed for the profile $\beta = 0.5\ km^{-1}$, $h' = 85$ km at 15.567 kHz. Both propagation models are seen to produce considerable interference structure throughout the range shown. The depth of the null which occurs close to 4 megameters is seen to be as great as 20 dB for both models. The differences in the signal level, between the two computations, is 12 dB at 4.2 megameters, and as much as 15 dB at 5.7 megameters. The curves are generally similar in appearance, and if the WAVEHOP fields were to be shifted inward by approximately 200 km, the agreement between the two computations would be much improved; however, some dissimilarities would remain. In particular the shapes of the nulls obtained from the two programs at approximately 2.5 and 4.0 megameters would not produce exact duplication.

The field strength comparison for the $\beta = 0.5\ km^{-1}$, $h' = 85$ km at 28.125 kHz is represented in Fig. 14. The signal levels of the two models are very similar throughout the propagation range. The deviation at 4.2 km is found to be 2 dB. In contrast to the daytime profile $\beta = 0.5\ km^{-1}$, $h' = 70$ km, where a much deeper mode structure was found for the 28.125-kHz signal than for the 15.567-kHz signal, this profile, which is a fair approximation of the electron densities expected at night, shows the greatest mode structure at the lower of the two frequencies. In fact, the interference structure at 8.0 megameters for 15.567 kHz is very significant, whereas for 28.125 kHz at 8.0 megameters mode interference appears to be quickly approaching a range where its effect will be negligible to the total field.

Figures 15 and 16 portray the fields computed by the WAVEHOP and WAVEGUIDE propagation models for the $\beta = 0.5\ km^{-1}$, $h' = 90$ km profile. In Fig. 15 the modal interference structure is shown to be very strong throughout the range for 15.567 kHz. A close observation of the $h' = 90$-km curves verifies that the two computations yield similar signal-level characteristics throughout the range. In particular, both models yield deep, narrow nulls at approximately 1.25 megameters, narrow relative maximums at about 1.75 megameters, and somewhat similar nulls at 2.75-3.0, 4.50-4.75, and 6.25-6.50 megameters. Also, the relative maximums have the same general shape at all ranges. The discrepancies between field-strength values obtained from the two computation methods for a given range can be very great. The differences are found to be 6 dB at 4.2 megameters, and as great as 18 dB at 6.25 megameters. Again, if the WAVEHOP field levels could be shifted inward in range by an interval of 200 to 250 km, the comparison of the

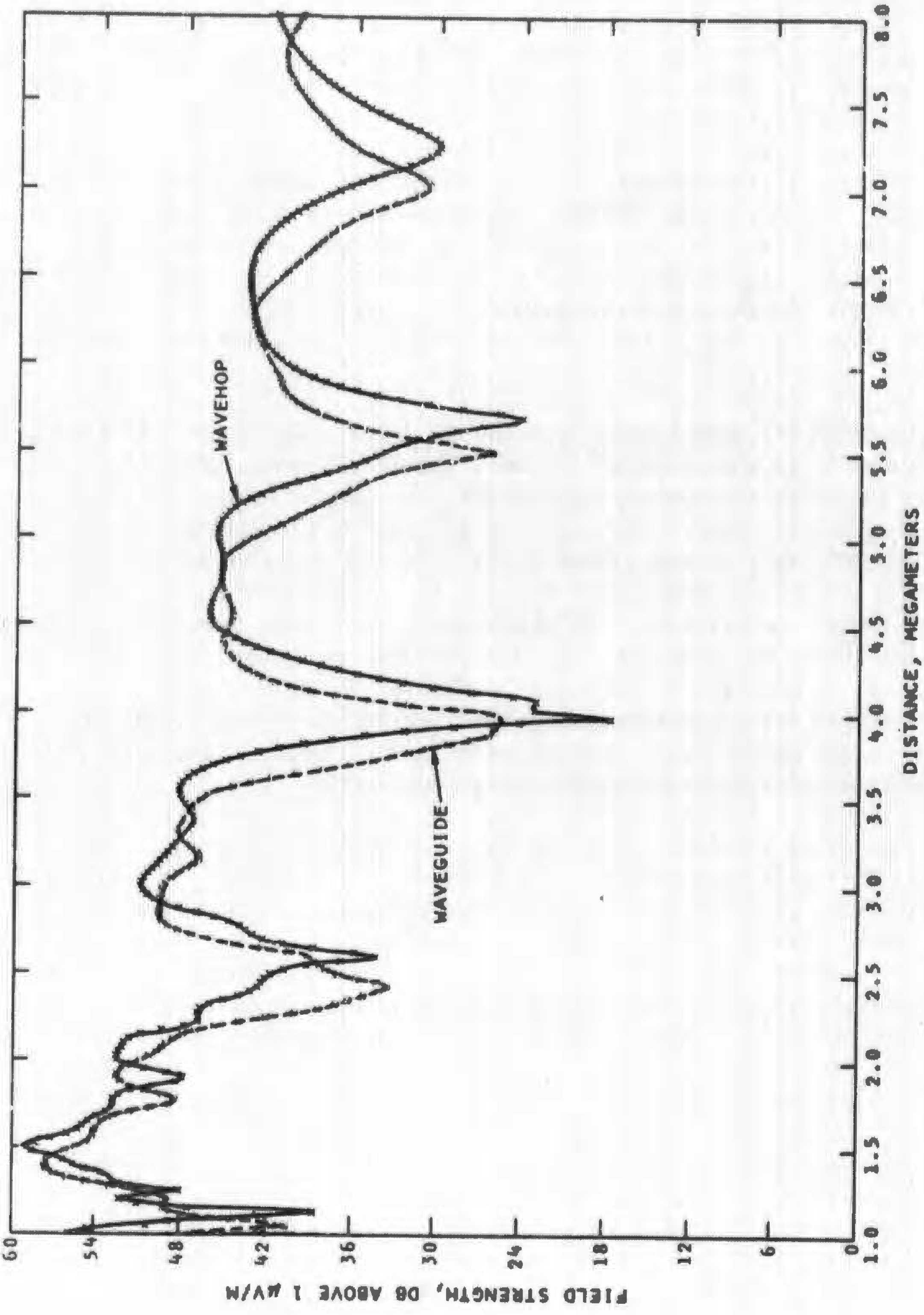

FIG. 13. Field Strength Versus Distance for WAVEHOP and WAVEGUIDE Comparison at 28.125 kHz ($\beta = 0.5\ km^{-1}$, $h' = 85$ km).

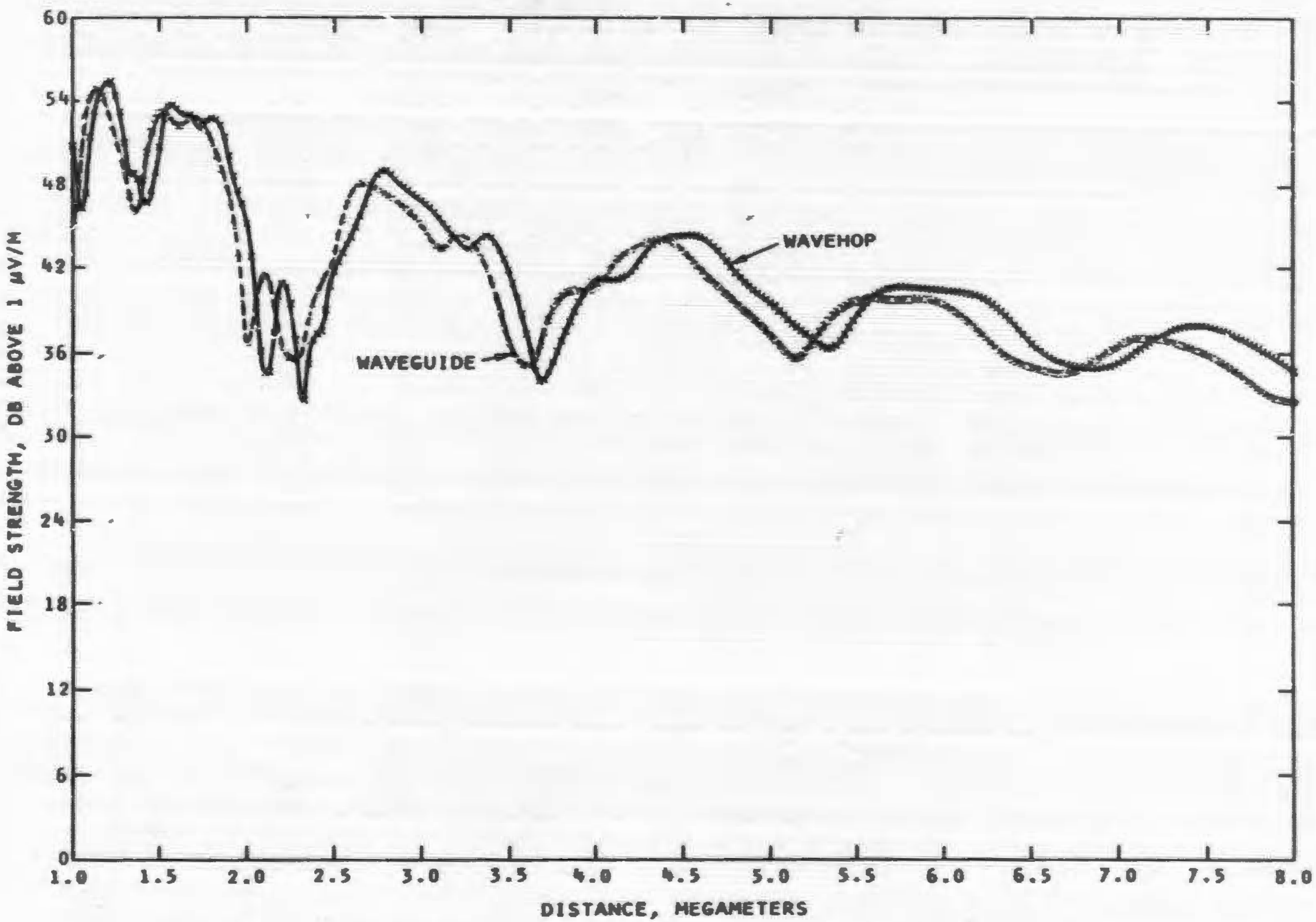

FIG. 14. Field Strength Versus Distance for WAVEHOP and WAVEGUIDE Comparison at 28.125 kHz ($\beta = 0.5\ km^{-1}$, $h' = 85\ km$).

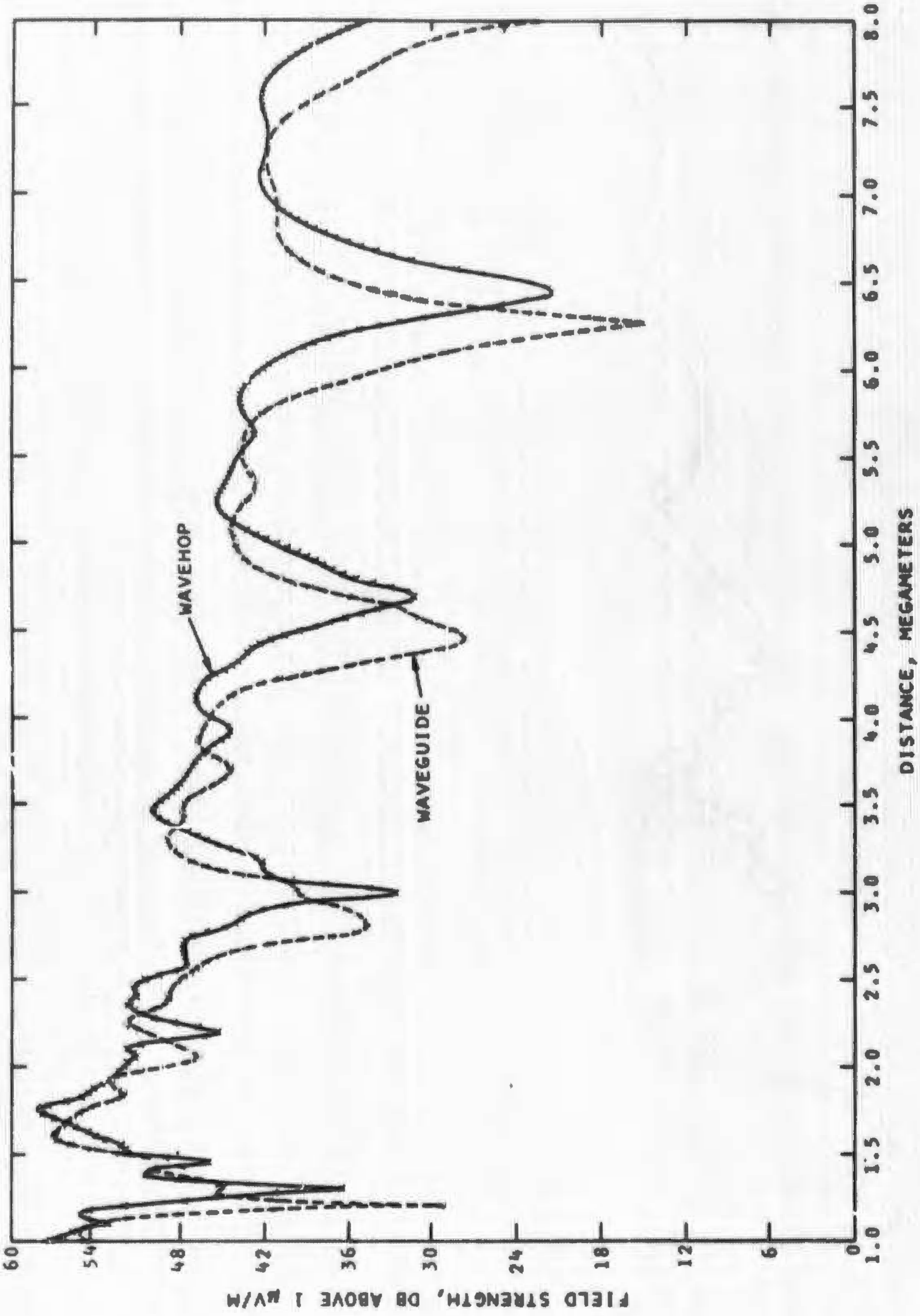

FIG. 15. Field Strength Versus Distance for WAVEHOP and WAVEGUIDE Comparison at 15.567 kHz (β = 0.5 km^{-1}, h' = 90 km).

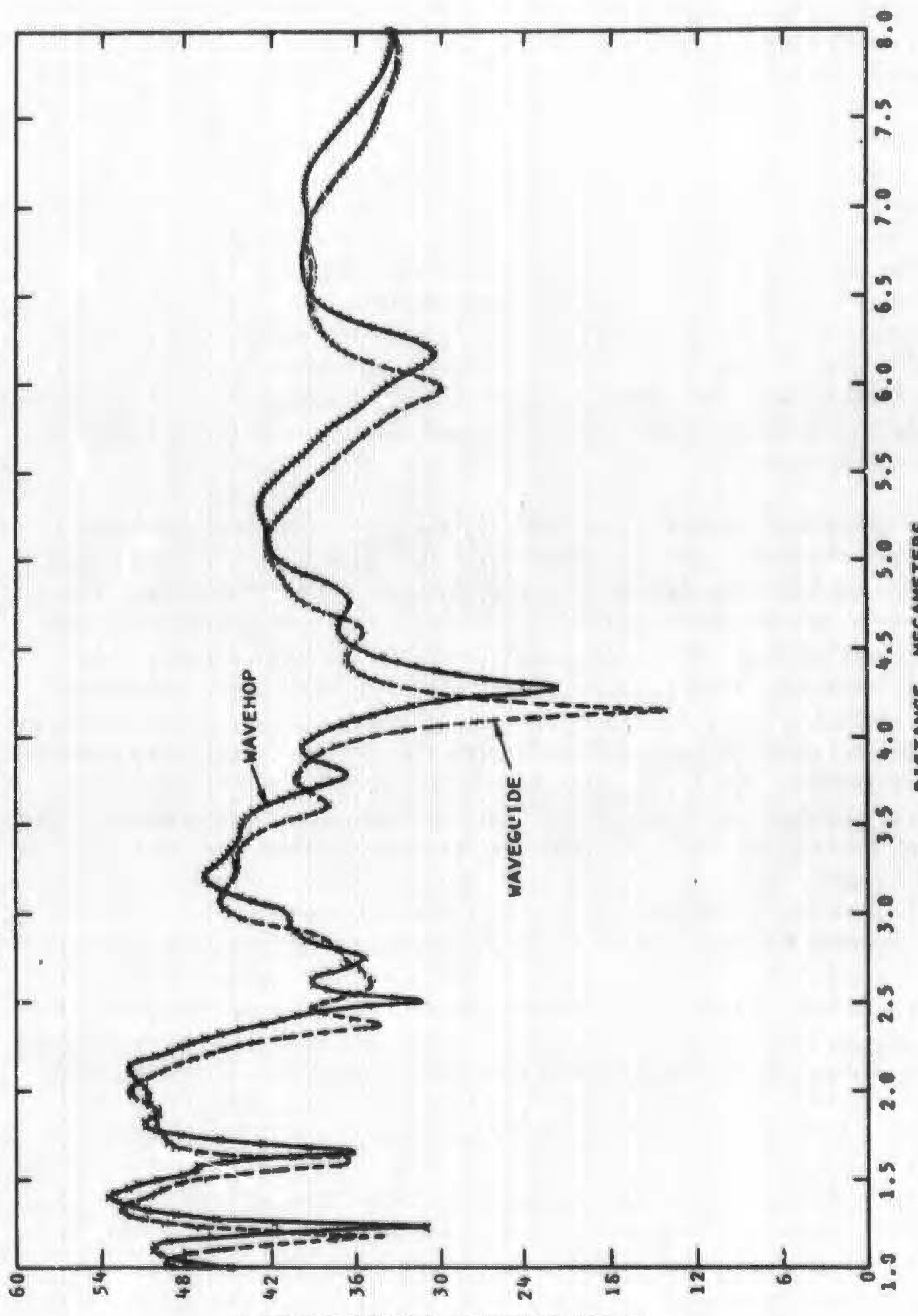

FIG. 16. Field Strength Versus Distance for WAVEHOP and WAVEGUIDE Comparison at 28.125 kHz (β = 0.5 km^{-1}, h' = 90 km).

fields computed by WAVEHOP and WAVEGUIDE would be much improved, although the exact shape and depth of the nulls would still not be identical.

Figure 16 shows the field computations at 28.125 kHz for the profile $\beta = 0.5$ km^{-1}, h' = 90 km. The two computation models produce a similar field strength pattern with range, but the actual field strength levels at a given range may be drastically different because of the apparent shift with distance between the two computations. In particular, the difference in signal level determined by the two methods is as much as 19 dB at 4.2 megameters. It is apparent from Fig. 16 that if the field values computed with WAVEHOP could be transformed inward approximately 200-250 km then the field levels computed as a function of propagation range would line up almost exactly with those computed by WAVEGUIDE.

In order to determine why the differences in the field patterns exist, the electron density in the WAVEHOP model was first lowered by 1 km, as was done for the $\beta = 0.5$ km^{-1}, h' = 70 km profile. The result was that the fields obtained for the h' = 90-km profile from the two models had a greater similarity, but still did not coincide. A further lowering of the profile used in WAVEHOP of 2 km yielded the field-strength results as shown in Fig. 17 where the agreement between the field-strength levels computed using the two computer programs is much improved. An adjustment of -1.5 km would probably give the optimum comparison between the two computations. Apparently, if the profiles as used in the WAVEHOP model are adjusted downward in height by some optimum amount, the two propagation models can be made to provide resultant fields with much more similarity. However, as the models presently exist, the resulting field strength levels obtained as a function of propagation distance can give drastically different results for a particular receiver range. The major ramification of this fact, in relation to the ionosphereic studies being conducted at the Corona Annex, is that a different ionospheric electron-density profile would be needed to fit experimentally recorded data, depending on whether WAVEHOP or WAVEGUIDE were being used in the investigation.

The reason for the discrepancies between the field strengths calculated by the two computer programs is not fully understood at this time. The results of Fig. 8 and 17 show that much improvement in the agreement between the two computations is achieved by lowering the ionospheric electron-density profile used as an input to the WAVEHOP program. An explanation as to the reason that this procedure gives field-

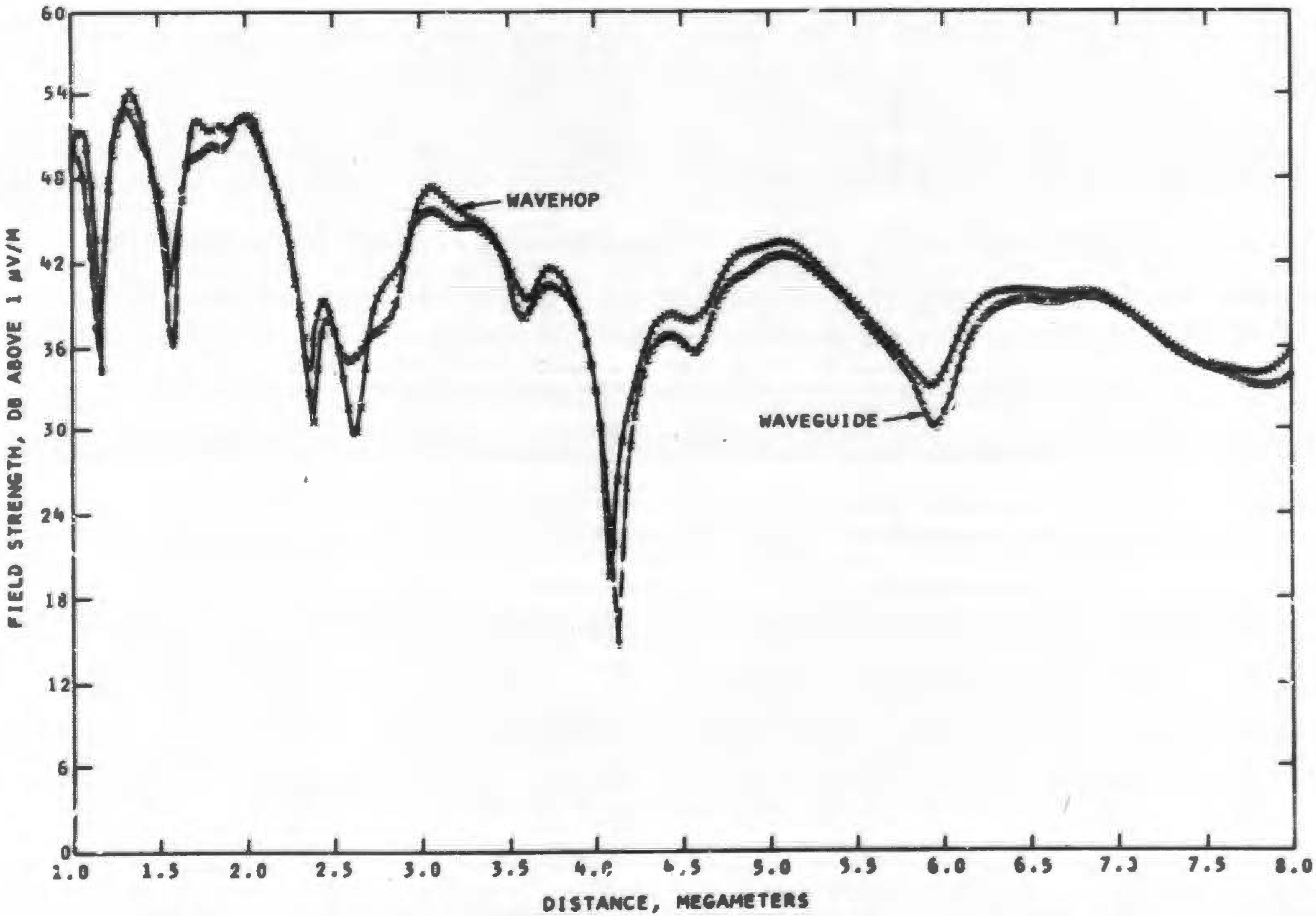

FIG. 17. Field Strength Versus Distance for WAVEHOP (β = 0.5 km^{-1}, h' = 90 km - 2.0 km) and WAVEGUIDE (β = 0.5 km^{-1}, h' = 90 km) Comparison at 28.125 kHz.

strength values which compare favorably with those obtained from WAVEGUIDE is possibly related to the method used within each of the computer programs to determine ionospheric reflection coefficients.

In the computer program TUIK, which is used to compute reflection coefficients for the WAVEHOP propagation model, the continuous ionosphere is approximated by one that is stratified, where the input electron-density profile is divided up into a series of equally spaced layers, each of which is considered to be homogeneous throughout. The electron density of any layer is then assumed to be that of the midpoint. The value of collision frequency corresponding to a particular layer is also assigned the value at the midpoint. These midpoint values of electron density and collision frequency are then used in a procedure which matches the upgoing and downgoing wave fields at each layer boundary. The method used computes the fields at the highest layer and then couples the results into each successively lower layer until the bottom of the profile is reached. At this height the reflection coefficients characteristic of the particular electron-density profile and propagation frequency are determined. Layer widths of less than 0.5 km for daytime and 0.75 km for nighttime are usually sufficient to satisfy the required convergence criteria (see Ref. 4).

In the WAVEGUIDE program, the modal differential equation is integrated by a Runge-Kutta technique starting at some height above which negligible reflection is assumed to take place. The integration is carried through the ionosphere using a variable step size dependent on how rapidly the reflection coefficients at each step change with height. The size of these steps reaches values of 0.01 km at the point of reflection, and in so doing, the density profile more closely approximates a continuously varying ionosphere than is found by using the TUIK method.

Because of the existing differences in layer (or slab) thickness used in the two models, further computations using TUIK at smaller layer increments were attempted. Slab widths of 0.1 km, which are the smallest possible with the Corona Annex version of the computer program, did not result in any improvement in agreement between the fields obtained from WAVEHOP and WAVEGUIDE. Further study will be required if the discrepancies in signal level computed by the two propagation models are to be explained and corrected.

CONCLUSIONS

In general, it is apparent that the ESSA WAVEHOP and the NELC WAVEGUIDE computerized propagation models, as they now exist, do not produce exactly the same computational results when using the same input parameters. The degree of difference in the computed field-strength levels is found to be dependent upon the propagation frequency and the input electron-density profile. The field-strength levels computed by the two programs have been shown in some instances to differ considerably when they are compared at a particular propagation distance. The significance of the discrepancy between the two computational methods depends on how the signal-level results are to be used. In some VLF communications applications where the field strength versus distance relationship is not needed in detail, either program may be used with an equal degree of confidence. However, for studies pertaining to the determination of characteristics of the propagation media, a precise knowledge of the relationship between field-strength level and propagation distance is required.

Investigations presently being made at the Corona Annex to determine the electron-density profile which exists over a given propagation path for a given time interval throughout the day and/or night are strongly dependent upon the detail which exists for signal levels as a function of propagation range. For the Corona studies, the fields computed by the propagation model are used in conjunction with experimentally recorded VLF data by comparing the computed and measured signal levels as obtained at a particular distance from the transmitter. Differences in the field strengths as computed by the WAVEHOP and WAVEGUIDE computer programs of 2 dB and greater at the 4.2 megameter range, as described in this report, result in the determination of two unequivalent electron-density profiles being characteristic of the ionosphere during the period for which the experimental data was acquired.

The original objective of this investigation was to determine which of the two computational methods was the more suitable for use in the interpretation of the VLF multifrequency propagation data being acquired at the Corona Annex in terms of computer efficiency, cost, and ease of operation. These original factors are now outweighed by the evident differences in computational results. Temporarily ignoring this factor and addressing the original objectives, it has been determined that use of the WAVEGUIDE method can be more economical for certain types of computations if the eigenangles needed for the modal solution can be found without extensive searching. Finding solutions for eigenangles is a trial and error process which for the inexperienced user can be difficult and time-consuming. The resulting computer costs are directly dependent upon this procedure. Because of this factor, direct comparison of costs with the WAVEHOP calculations is very difficult and cannot be quantitatively expressed at this time, except to indicate that the WAVEGUIDE results could easily straddle the WAVEHOP costs, varying from significantly less to significantly greater, depending upon the skill of the operator.

A note of caution is considered in order regarding the use of either of these programs by the "non-expert" investigator. Indiscriminate use of either program by inexperienced personnel without close communication with originators is not recommended. Erroneous results from improper operation of WAVEGUIDE and WAVEHOP programs could occur.

It has been the experience at the Corona Annex that the adaptation and use of WAVEHOP is more straightforward and that it requires less skill to use, and the operator is less likely to miss an important signal component in the vector summation process. In view of the differences in computational results, it is evident that a further investigation is warranted in terms of general theory, approximations used in the theory, and special computational techniques used for computer adaptation. The initial approach to this investigation should be to make appropriate, comparative calculations which would clearly illustrate the source of the differences. If these differences cannot be easily explained on the basis of techniques, a propagation experiment could be designed which would make it possible to test the representativeness of either model. It is also important to carefully select the frequencies and distances that would produce the greatest discrimination between the two models.

Appendix

CORRECTIONS TO THE WAVEHOP PROGRAM

In the original development of the wave-hop propagation model (Ref. 3 and 4) the jth wave-hop term was computed as

$$E_j = \gamma_j I_j \tag{1}$$

where γ_j is the effective ionospheric reflection coefficient for a plane, stratified, anisotropic ionosphere, and I_j is a path integral which accounts for the effects of ground conductivity, reflection, height, earth curvature, and propagation range. In the following Eq. 2, γ_j is computed from:

$$\begin{pmatrix} \gamma_j & a_{12} \\ a_{21} & a_{22} \end{pmatrix} = \begin{pmatrix} T_{ee} & T_{em} \\ -R_m T_{me} & -R_m T_{mm} \end{pmatrix}^j \tag{2}$$

where

R_m = the Fresnel ground reflection coefficient for horizontal polarization

T_{ee} = the ratio of the incident field in the plane of incidence to the reflected field in the same plane

T_{mm} = the ratio of the incident field perpendicular to the plane of incidence to the reflected field perpendicular to the plane of incidence

T_{em} = the ratio of the incident field in the plane of incidence to the reflected field perpendicular to it

T_{me} = the ratio of the incident field perpendicular to the plane of incidence to the reflected field in the plane of incidence

It has recently been established, however, that the original version of the wave-hop theory contained several limitations and inaccuracies that were not previously recognized or fully appreciated. In particular, the formulation of the effective ionospheric reflection coefficient for the second and higher order hops was incorrect for an anisotropic ionosphere. The corrected equation should read (see Ref. 17):

$$E_r = E_o + \sum_{j=0}^{N} E_j \tag{3}$$

where

E_o = the ground wave

E_j = the field for the jth wavehop

N = the number of wavehops

For j = 1,

$$E_1 = \int F_j(t) T_{ee} dt \tag{4}$$

For j > 1,

$$E_j = \int F_j(t) \left(a_j T_{ee} + C_j T_{em} \right) dt \tag{5}$$

where

$$a_j = R_e \left(T_{ee} a_{j-1} + T_{em} C_{j-1} \right) \tag{6}$$

$$C_j = R_m \left(T_{me} a_{j-1} + T_{mm} C_{j-1} \right) \tag{7}$$

with $a_1 = 1$, $C_1 = 0$, also

R_e = the Fresnel ground reflection coefficient for vertical polarization

F_j = a new function of the propagation path

The deficiencies in the model have been corrected and the individual wavehops are now calculated with the proper formulation of the effective ionospheric reflection coefficient.

The error was not found to be significant for daytime propagation, at least at the ranges used by the Corona Annex for the Hawaii to Southern California propagation path. This is not the case for nighttime propagation where the computations were found to be in considerable error. Comparisons of the electric fields computed using the original version of WAVEHOP (see Ref. 4) and the corrected version are illustrated in Fig. 18 and 19 for a propagation path over sea water. In these figures the computations obtained using the original WAVEHOP are plotted as WAVEHOP (original) while the corrected values are plotted as WAVEHOP (corrected).

Figure 18 shows the daytime comparison for the profile $\beta = 0.5$ km^{-1}, $h' = 70$ km for 28.125 kHz. It is observed that the values compare favorably out to about 4.5 megameters. At greater distances the degree of comparison reduces quickly, especially in the vicinity of the field nulls. It is important to notice that the two computational methods agree at the Hawaii to Southern California propagation range of 4,200 km. Because of this, the results obtained in previous Corona Annex reports for daytime propagation remain valid (see Ref. 5 and 6).

Figure 19 for 28.125 kHz illustrates the nighttime comparison for the profile $\beta = 0.5$ km^{-1}, $h' = 90$ km. It is seen in this comparison that the results from the two computational methods vary drastically. The publications (Ref. 7 and 8) for nighttime comparison were written using the corrected version of WAVEHOP, so the results were valid.

In the original version of the WAVEHOP program, the path integral I_j of Eq. 1 was evaluated by one of three methods, depending on propagation range relative to the position of the caustic. In general, the saddle-point approximation was used to evaluate the integral in the lit region of the propagation path except near the caustic; numerical integration was used in the vicinity of the caustic on the lit side, and a residue series was used in the shadow region.

In the corrected version of the WAVEHOP computer program, the above methods may again be used to evaluate the integrals in Eq. 4 and 5. In the shadow region, however, the integrals can also be evaluated by substituting numerical integration for the residue series expansion. Due to the complexity of solving the integrals of Eq. 5 by the residue

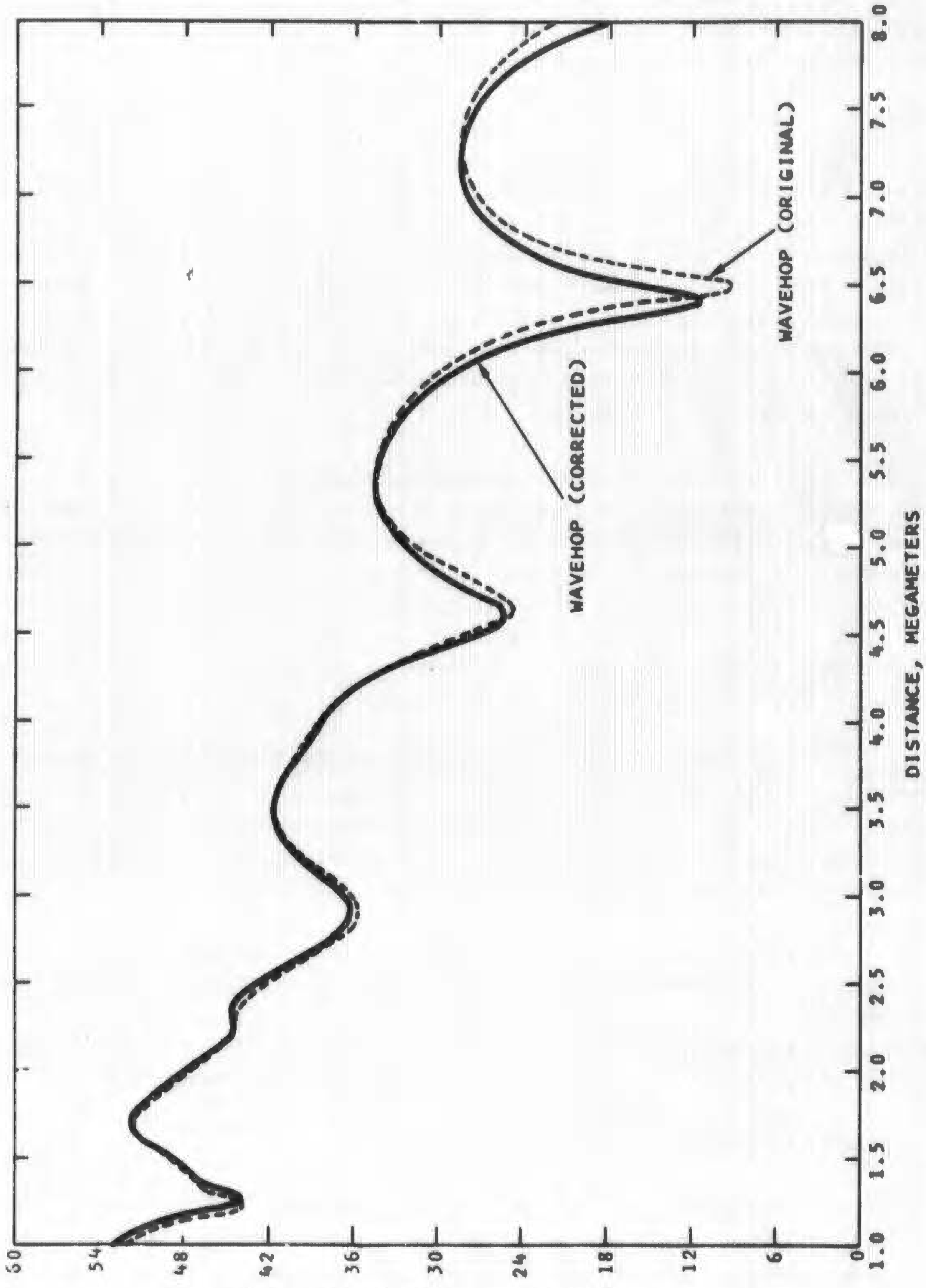

FIG. 18. Field Strength Versus Distance for WAVEHOP (corrected) and WAVEHOP (original) Comparison at 28.125 kHz (β = 0.5 km^{-1}, h' = 70 km).

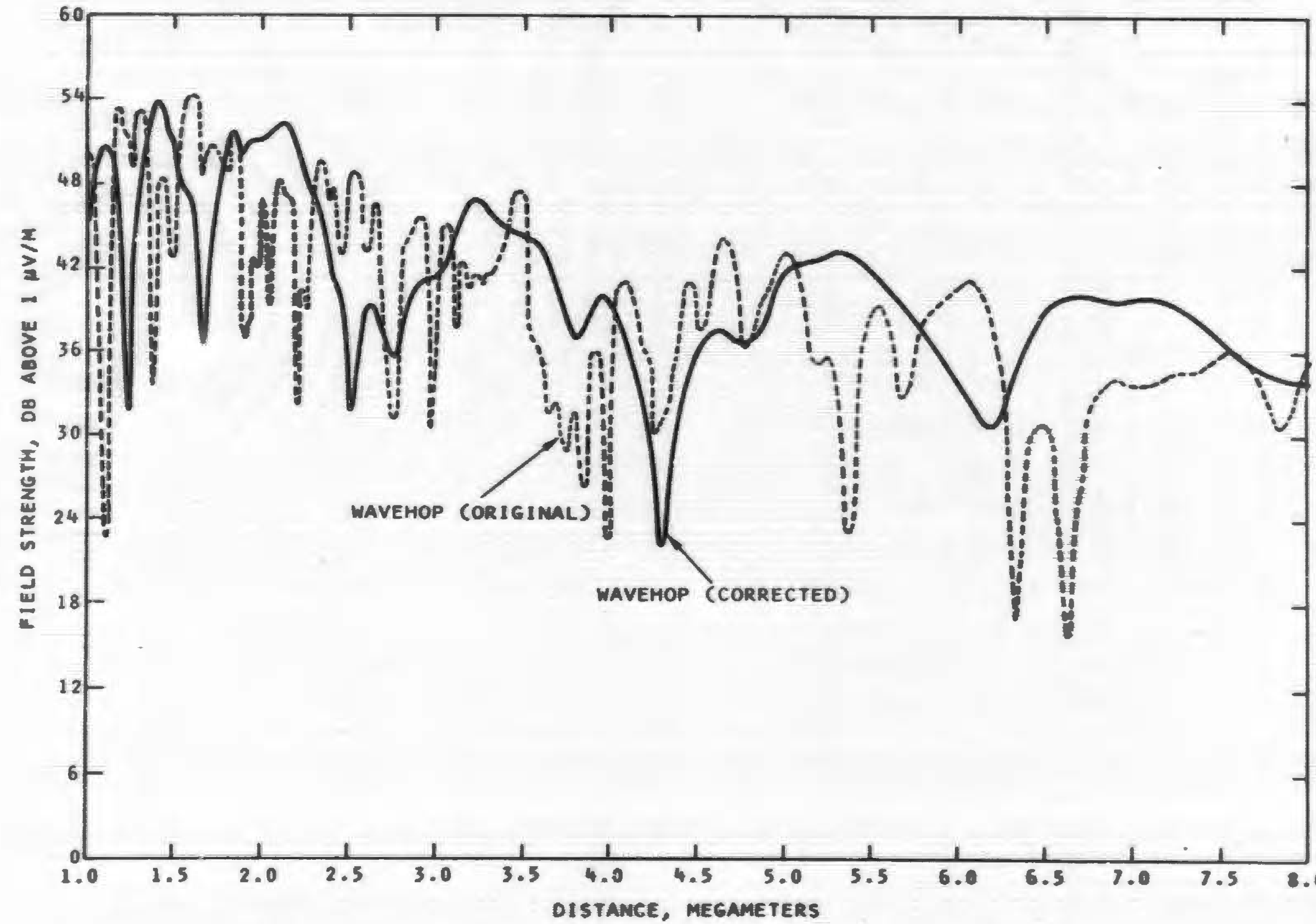

FIG. 19. Field Strength Versus Distance for WAVEHOP (corrected) and WAVEHOP (original) Comparison at 28.125 (β = 0.5 km^{-1}, h' = 90 km).

method, the numerical integration equations and computer program corrections were developed[1] and implemented into the WAVEHOP program. Thus, the correct field strengths, as computed by WAVEHOP in this report, were obtained using the numerical integration method.

A corrected version of WAVEHOP where the residue series is again incorporated into the program is presently being prepared and will be available soon.[2] This residue series program will be approximately three times faster than the numerical integration version presently being used at the Corona Annex.

[1] Private communication with L. A. Berry of the Institute for Telecommunication Sciences and Aeronomy, Environmental Science Services Administration, Boulder, Colorado, dated May 1969.

[2] Private communication as cited in footnote 1, dated January 1970.

REFERENCES

1. Naval Ordnance Laboratory, Corona. Multiple-Frequency Oblique Incidence VLF Ionosphere Sounder, by V. E. Hildebrand and D. A. Wulfing. Corona, Calif., NOLC, 5 May 1967. (NOLC Report 722.)

2. Defense Atomic Support Agency. Summary of VLF and LF Computer Codes. Santa Barbara, Calif., General Electric Company, November 1968. (DASA Report 2212.)

3. Berry, L. A. "Wavehop Theory of Long Distance Propagation of Low-Frequency Radio Waves," NAT BUR STAND, J. RES, SECT D, RADIO SCI, Vol. 68D, No. 12 (December 1964), pp. 1275 - 1284.

4. National Bureau of Standards. FORTRAN Programs for Full-Wave Calculation of LF and VLF Radio Propagation, by L. A. Berry and M. E. Chrisman. Boulder, Colo., NBS Boulder Laboratories, 11 October 1965. (NBS Report 8889.)

5. Naval Weapons Center Corona Laboratories. An Evaluation of VLF Daytime Propagation Parameters Using a Multi-Frequency Sounder, by V. E. Hildebrand and D. G. Morfitt. Corona, Calif., NWC Corona Laboratories, March 1968, p. 7. (NWCCL TP 75?.)

6. Naval Weapons Center Corona Laboratories. Computations of VLF Fields for Determination of Electron Density Profiles Using Oblique Sounder Data, by D. G. Morfitt and V. E. Hildebrand. Corona, Calif., NWC Corona Laboratories, October 1968. (NWCCL TP 806.)

7. Naval Weapons Center Corona Laboratories. A Nighttime Ionospheric Profile Matching for 1030 U.T., by D. G. Morfitt and V. E. Hildebrand. Corona, Calif., NWC Corona Laboratories, May 1969. (NWCCL TP 829.)

8. Naval Weapons Center Corona Laboratories. Examination of VLF/LF Propagation Effects as a Function of Frequency, by V. E. Hildebrand and D. G. Morfitt. Corona, Calif., NWC Corona Laboratories, December 1969. (NWCCL TP 886.)

9. Naval Electronics Laboratory Center. A FORTRAN Program for Mode Constants in an Earth-Ionosphere Waveguide, by C. H. Sheddy, R. Pappert, Y. Gough, and W. Moler. San Diego, Calif., NELC, 31 May 1968. (Interim Report No. 683.)

10. Pappert, R. A., E. E. Gossard, and I. J. Rothmuller. "A Numerical Investigation of Classical Approximations Used in VLF Propagation," RADIO SCIENCE, Vol. 2, No. 4 (April 1967) pp. 387-400.

11. Pappert, R. A. "A Numerical Study of VLF Mode Structure and Polarization Below an Anisotropic Ionosphere," RADIO SCIENCE, Vol. 3, No. 3 (March 1968), pp. 219-233.

12. Snyder, F. P., and R. A. Pappert. "A Parametric Study of VLF Modes Below Anisotropic Ionospheres," RADIO SCIENCE, Vol. 4, No. 3 (March 1969), pp. 213-226.

13. National Bureau of Standards Boulder Central Radio Propagation Laboratory. Characteristics of the Earth-Ionosphere Waveguide for VLF Radio Waves, by J. R. Wait and K. P. Spies. Washington D. C., Government Printing Office, 30 Dec. 1964. (NBS Technical Note No. 300.)

14. Bickel, J. F., J. A. Ferguson, and G. V. Stanley. "Experimental Observation of Magnetic Field Effects on VLF Propagation at Night," RADIO SCIENCE, Vol. 5, No. 1 (January 1970), pp. 19-25.

15. Field, E. C., and R. D. Engel. "The Detection of Daytime Nuclear Bursts Below 150 km by Prompt VLF Phase Anomalies," INST ELEC ELECTRON ENG, PROC, Vol. 53, No. 12 (December 1965), pp. 2009-2017.

16. Wait, J. R. Electromagnetic Waves in Stratified Media. New York, The Macmillan Company, 1962. pp. 224-225.

17. Berry, L. A., G. Gonzalez, and John L. Lloyd. "Wave-hop Series for an Anisotropic Ionosphere," RADIO SCIENCE, Vol. 4, No. 11 (November 1969), pp. 1025-1027.

Security Classification UNCLASSIFIED

DOCUMENT CONTROL DATA - R & D

(Security classification of title, body of abstract and indexing annotation must be entered when the overall report is classified)

1. ORIGINATING ACTIVITY (Corporate author) Naval Weapons Center China Lake, California	2a. REPORT SECURITY CLASSIFICATION UNCLASSIFIED 2b. GROUP

3. REPORT TITLE

COMPARISON OF WAVEGUIDE AND WAVEHOP TECHNIQUES FOR VLF PROPAGATION MODELING

4. DESCRIPTIVE NOTES (Type of report and inclusive dates)

5. AUTHOR(S) (First name, middle initial, last name)

David G. Morfitt
R. F. Halley

6. REPORT DATE	7a. TOTAL NO. OF PAGES	7b. NO. OF REFS
June 1970	58	17

8a. CONTRACT OR GRANT NO.	9a. ORIGINATOR'S REPORT NUMBER(S)
b. PROJECT NO. DASA MIPR 545-70	NWC TP 4952
c.	9b. OTHER REPORT NO(S) (Any other numbers that may be assigned this report)
d.	

10. DISTRIBUTION STATEMENT

THIS DOCUMENT IS SUBJECT TO SPECIAL EXPORT CONTROLS AND EACH TRANSMITTAL TO FOREIGN GOVERNMENTS OR FOREIGN NATIONALS MAY BE MADE ONLY WITH PRIOR APPROVAL OF THE OFFICER IN CHARGE OF THE NAVAL WEAPONS CENTER CORONA LABORATORIES (CODE 7565), CORONA, CALIFORNIA 91720.

11. SUPPLEMENTARY NOTES	12. SPONSORING MILITARY ACTIVITY
	Defense Atomic Support Agency Washington, D. C. 20301

13. ABSTRACT

Several mathematical models for describing VLF radio wave propagation in the earth-ionosphere waveguide have been presented in the literature. The Wave Hop model and the Waveguide mode model are investigated.

The computerized versions of these propagation models are examined by comparing the computed electric field strengths obtained for each model when using the same input parameters. It is found that the two models as they now exist do not produce exactly the same computational results and the degree of difference between the two computations is dependent upon propagation frequency and the electron density profile used for the ionosphere.

DD FORM 1 NOV 65 1473 (PAGE 1)

S/N 0101-807-6801

UNCLASSIFIED
Security Classification

Security Classification UNCLASSIFIED

14 KEY WORDS	LINK A		LINK B		LINK C	
	ROLE	WT	ROLE	WT	ROLE	WT
VLF radio-wave propagation Wave-hop theory WAVEHOP propagation model WAVEGUIDE propagation model Mode theory						

DD FORM 1 NOV 65 1473 (BACK)
(PAGE 2)

UNCLASSIFIED
Security Classification